



Theses and Dissertations

2021-06-04

Remote Sensing and Spatial Variability of Leaf Area Index of Irrigated Wheat Fields

Austin Paul Hopkins
Brigham Young University

Follow this and additional works at: <https://scholarsarchive.byu.edu/etd>



Part of the [Life Sciences Commons](#)

BYU ScholarsArchive Citation

Hopkins, Austin Paul, "Remote Sensing and Spatial Variability of Leaf Area Index of Irrigated Wheat Fields" (2021). *Theses and Dissertations*. 9523.
<https://scholarsarchive.byu.edu/etd/9523>

This Thesis is brought to you for free and open access by BYU ScholarsArchive. It has been accepted for inclusion in Theses and Dissertations by an authorized administrator of BYU ScholarsArchive. For more information, please contact ellen_amatangelo@byu.edu.

Remote Sensing and Spatial Variability of Leaf Area Index of Irrigated Wheat Fields

Austin Paul Hopkins

A thesis submitted to the faculty of
Brigham Young University
in partial fulfillment of the requirements for the degree of

Master of Science

Neil Hansen, Chair
Ryan Jensen
Bradley Geary

Department of Plant and Wildlife Sciences

Brigham Young University

Copyright © 2021 Austin Paul Hopkins

All Rights Reserved

ABSTRACT

Remote Sensing and Spatial Variability of Leaf Area Index of Irrigated Wheat Fields

Austin Paul Hopkins
Department of Plant and Wildlife Sciences, BYU
Master of Science

Leaf area index (LAI) is a versatile indicator of crop growth that is used to estimate evapotranspiration (ET), monitor nitrogen status, and estimate crop yield. Traditional methods for measuring LAI can be improved using high resolution remote sensing. The aim of this study was to compare approaches for estimating LAI from UAV-derived visible vegetation indices. Coincident ground-based and remotely sensed data were obtained from two irrigated wheat fields and were sampled at a total of 5 events in 2019 and 2020. Ground-based LAI was measured with a ceptometer and remotely sensed images were collected using a consumer-grade UAV. Mosaiced orthophotos were resampled from native (0.06m) spatial resolution to increasingly coarser spatial resolutions up to 3 m by either a direct or ladder resampling method. Visible band color information (RGB) was extracted from the orthophotos at the points that LAI was collected within field and 12 different visible vegetation indices (VVI) were calculated. Linear regression was performed to evaluate the relationships between wheat LAI and each calculated VVI for all spatial resolutions and resampling methods. Three VVIs, visible atmospherically resistant index (VARI), normalized green-red difference index (NGRDI), and modified green-red vegetation index (MGRVI), estimated LAI equally well ($R^2=0.66, 0.66, 0.66$; $RMSE=0.74, 0.73, 0.73$; $MAE=0.57, 0.56, 0.56$) when resampled to 3 m spatial resolution with the ladder resampling method. These results demonstrate the potential to remotely estimate LAI using only RGB cameras and consumer grade drones. An additional aim of this study was to evaluate use of a remotely sensed visible vegetation index to characterize the spatial variability of LAI within irrigated wheat fields. A visible atmospherically resistant index (VARI) LAI estimation model was applied to red, green, blue (RGB) UAV imagery using a ladder resampling approach from 0.06 m to 3 m spatial resolution. There was significant within-field spatial and temporal variation of mean LAI. For example, in May at the Grace, ID location measured LAI ranged from 0.21 to 2.58 and in June from 1.68 to 4.15. The relationship of measured and estimated LAI among management zones was strong ($R^2=0.84$), validating the remote sensing approach to characterize LAI differences among management zones. There were statistically significant differences in estimated LAI among zones for all sampling dates ($P=0.05$). We assumed a minimum difference of 15% between zone LAI and the field mean for justifying variable rate irrigation among zones, a threshold that corresponds with approximately a 10% difference in evapotranspiration rate. Three of the five sampling dates had LAI differences that exceeded the threshold for at least one zone, with all three having mean LAI of less than 2.5. The VARI model for estimating LAI remotely is more effective at identifying LAI differences among management zones at lower LAI. Application of this approach has potential for applications such as estimating evapotranspiration of irrigated fields and delineation of zones for variable rate irrigation.

Keywords: leaf area index (LAI), remote sensing, variable rate irrigation, wheat, unmanned aerial vehicles, visible vegetation indices, precision agriculture

ACKNOWLEDGEMENTS

I would like to acknowledge all the people that influenced me in pursuing this degree. I appreciate all the students, teachers and volunteers who lent me their valuable time in accomplishing this work. I appreciate my family and friends and their endless support.

I would like express my gratitude to my wife Karenn, and my children, I could not have accomplished this without them. I would also like to thank my committee for providing excellent guidance, vision, and strength. Thank you to Dr .Neil Hansen for all the guidance he has provided me. My gratitude also goes to Dr. Ryan Jensen and Dr Ruth Kerry for their excellent teaching, and Dr Brad Geary for his help. I want to thank Ryan Christensen for partnering with us and allowing us to work on his land. I want to thank my mother Carrie Hopkins and my father Bryan Hopkins for all they did and do to help me get to where I am now. I hope my work inspires my children to always pursue the difficult paths in life in order to garner strength from them.

TABLE OF CONTENTS

TITLE PAGE	i
ABSTRACT.....	ii
ACKNOWLEDGEMENTS.....	iii
TABLE OF CONTENTS.....	iv
LIST OF FIGURES	vi
LIST OF TABLES.....	ix
CHAPTER 1	1
ABSTRACT	1
INTRODUCTION.....	2
MATERIALS AND METHODS	5
Site Description	5
Leaf Area Index Measurements.....	7
RESULTS.....	11
Variability of Wheat Leaf Area Index.....	11
Evaluation of Visible Vegetation Indices, Resolution, and Resampling Methods.....	12
DISCUSSION	13
Visible Vegetation Index Comprehensive Performance For Wheat Leaf Area Index Estimation.....	13
Spatial Resolution Results.....	14
CONCLUSION	17
LITERATURE CITED	18

FIGURES	24
TABLES	36
SUPPLEMENTAL MATERIAL	40
CHAPTER 2	41
ABSTRACT	41
INTRODUCTION.....	42
MATERIALS AND METHODS	45
Site Description	45
UAV Image Acquisition and Processing.....	46
Leaf Area Index Measurement and Estimation.....	47
RESULTS.....	50
Spatial and Temporal Variability of Measured Wheat Leaf Area Index.....	50
Spatial and Temporal Variability of Estimated Leaf Area Index.....	51
Management Zone Comparisons of Measured and Estimated Leaf Area Index.....	53
DISCUSSION	55
Spatial and Temporal Variability of Measured and Estimated Leaf Area Index	55
Predefined Management Zone Differences Between Ceptometer Measured and Unmanned Aerial Vehicle Estimated Leaf Area Index.....	56
CONCLUSION	63
LITERATURE CITED	65
FIGURES	69
TABLES	76

LIST OF FIGURES

Figure 1-1 Leaf area index sample point locations in Rexburg, Idaho irrigated wheat field. 24

Figure 1-2 Leaf area index sample point locations in Grace, Idaho irrigated wheat field. 25

Figure 1-3 Traditional RGB orthophoto generated from images acquired over the Rexburg, ID winter wheat study location on 25 June 2019. The images were acquired with a DJI Phantom 4 flying 300 feet above ground level and processed with Web OpenDroneMap. 26

Figure 1-4 Model depicting the ladder and direct resampling method. Direct resampling takes an image in the native resolution and resizes it directly to the desired resolution. Ladder resampling takes an image in the native resolution and resizes gradually through coarser resolutions. 27

Figure 1-5 Coefficient of determination (R^2) values for the correlations of 12 visible vegetation indices (VVI) with pooled data of measured wheat leaf area index over five sampling events. 28

Figure 1-6 Root Mean Square Error (RMSE) values from simple linear regression models of 12 visible vegetation indices (VVI) with pooled data of measured wheat leaf area index over five sampling events. 29

Figure 1-7 Mean Absolute Error (MAE) values from simple linear regression models of 12 visible vegetation indices (VVI) with pooled data of measured wheat leaf area index over five sampling events. 30

Figure 1-8 Results of the comparison of Direct v Ladder resampling methods for VARI, NGRDI, and MGRVI at all spatial resolutions. This shows the variation in RMSE values for each model between the two resampling methods. 31

Figure 1-9 (a) Root mean square error values (RMSE) of the VVI- based simple linear regression models for wheat LAI estimation in May 2019, June 2019, and July 2020 in Grace Idaho at 1 meter spatial resolution derived with the Direct resampling method and (b) R^2 values between VVI and LAI. 32

Figure 1-10 (a) Root mean square error values (RMSE) of the VVI- based simple linear regression models for wheat LAI estimation in May 2019, June 2019, and July 2020 in Grace Idaho at 1 meter spatial resolution derived with the Ladder resampling method and (b) R² values between VVIs and wheat LAI. 33

Figure 1-11 (a) Root mean square error values (RMSE) of the VVI- based simple linear regression models for wheat LAI estimation across sampling dates, May 2019, and June 2019 in Rexburg Idaho at 3 meter spatial resolution derived with the Direct resampling method and (b) R² values between VVIs and wheat LAI. 34

Figure 1-12 (a) Root mean square error values (RMSE) of the VVI- based simple linear regression models for wheat LAI estimation across sampling dates, May 2019, and June 2019 in Rexburg Idaho at 3 meter spatial resolution derived with the Direct resampling method and (b) R² values between VVIs and wheat LAI. 35

Figure 2-1 Aerial image from a UAV and map of sample points where leaf area index was measured with a ceptometer at the Grace, Idaho location The inset figure shows the pre-determined management zones for this field. 69

Figure 2-2 Aerial image from a UAV and map of sample points where leaf area index was measured with a ceptometer at the Rexburg, Idaho location The inset figure shows the pre-determined management zones for this field. 70

Figure 2-3 Leaf area index of the Grace, Idaho field location measured using a ceptometer on a: May 30, 2019, b: June 25, 2019, c: July 8, 2020 and spatially interpolated using Kriging. 71

Figure 2-4 Leaf area index of the Rexburg, Idaho field location measured using a ceptometer on a: May 31, 2019 and b: June 26 and spatially interpolated using Kriging. 72

Figure 2-5 Raster images representing estimated LAI values for the Grace, Idaho field location on a: May 30 2019 b: June 25 2019 and c: July 8 2020 based on VARI model LAI estimation methods. 73

Figure 2-6 Raster image representing estimated LAI values for the Rexburg, Idaho field location on a: May 31 2019 and b: June 26 2019 based on VARI model LAI estimation methods. 74

Figure 2-7 Scatterplot with fit line (dotted) and a 1:1 line (solid), R2 value, and regression equation of the comparison of the mean leaf area index (LAI) measured for each zone to the mean LAI estimated using a model derived from images taken with an unmanned aerial vehicle (UAV) for each zone using data from all sampling dates and both locations 75

LIST OF TABLES

Table 1-1 Sampling dates, crop type, soil texture and crop growth stage for five UAV data collection events that occurring at two Idaho field locations. 36

Table 1-2 The abbreviations, names, formulas, and references for twelve visible vegetation indices (VVI) that were evaluated. 37

Table 1-3 Descriptive statistics of leaf area index (LAI) measured at two locations and five events including the number of samples, the minimum (min), maximum (max), mean, standard deviation (SD), and the coefficient of variation (CV). 38

Table 1-4 Model summaries for three leaf area index estimation models that predict leaf area index at the highest accuracy levels. 39

Table 2-1 Sampling dates, crop type, and soil texture for the two field locations. On these dates, LAI was measured on the ground using ceptometer readings and unmanned aerial vehicle (UAV) images were obtained for calculation of leaf area index. 76

Table 2-2 Descriptive statistics of measured leaf area index (LAI) and unmanned aerial vehicle (UAV) estimated LAI measured on multiple dates at the Grace, ID and Rexburg, ID locations. 77

Table 2-3 Estimated leaf area index (LAI) values for the Grace, ID location averaged by date and management zone and the percent difference between management zone and field means. Estimated LAI means followed by the same letter do not significantly differ. 78

Table 2-4 Estimated leaf area index (LAI) values for the Rexburg, ID location averaged by date and management zone and the percent difference between management zone and field means. Estimated LAI means followed by the same letter do not significantly differ. 79

CHAPTER 1

Visible Vegetation Indices Resolution and Resampling Methods for Modeling Leaf Area Index of Irrigated Wheat

Austin Paul Hopkins, Ryan Jensen, Bryan Hopkins, Elisa Woolley, Neil Hansen
Department of Plant and Wildlife Sciences, Brigham Young University, Provo, UT
Master of Science

ABSTRACT

Leaf area index (LAI) is an indicator of crop growth that is used to estimate evapotranspiration (ET), monitor nitrogen status, and estimate crop yield. Traditional methods for measuring LAI can be improved using high resolution remote sensing, especially when within-field spatial variation of LAI is wanted. The objective of this study was evaluate the relationship of LAI and VVIs and to identify the most accurate VVIs to estimate within-field variation of LAI using a consumer-grade UAV, determine the most suitable spatial resolution for remote estimation of within-field variability of LAI, and examine the most accurate resampling method at various spatial resolutions for describing spatial variation of LAI in an irrigated wheat field. Coincident ground-based LAI data and remotely sensed visible band imagery data were obtained from two irrigated wheat fields and were sampled at a total of 5 dates in 2019 and 2020. Ground-based LAI was measured with a ceptometer and remotely sensed visible imagery was collected using a consumer-grade UAV. Mosaiced orthophotos were resampled from native (0.06m) spatial resolution to increasingly coarser spatial resolutions up to 3 m by either a direct or ladder resampling method. Visible band color information (RGB) was extracted from the orthophotos at the points that LAI was collected within field and 12 different visible vegetation indices (VVIs) were calculated. Linear regression was performed to evaluate the relationships between wheat LAI and each calculated VVI for all spatial resolutions and resampling methods.

Three VVIs, visible atmospherically resistant index (VARI), normalized green-red difference index (NGRDI), and modified green-red vegetation index (MGRVI), estimated LAI to the same accuracy ($R^2= 0.66, 0.66,0.66$; $RMSE=0.74,0.73,0.73$; $MAE=0.57,0.56,0.56$) when resampled to 3 m spatial resolution with the ladder resampling method. Our results demonstrate the potential to remotely estimate LAI using only RGB cameras and consumer grade drones. We found that the measured LAI varied spatially within the fields as well as temporally through the growing season. The predicted LAI was effective at showing similar field means and spatial variation to the measured LAI values. In addition, the relationship between the predicted and measured LAI is more accurate at lower LAI wheat values than higher LAI values later in the growing season. This approach has potential for applications such as estimating evapotranspiration of irrigated fields and delineation of zones for variable rate irrigation systems.

INTRODUCTION

Leaf Area Index (LAI) is a measure of above ground leafy growth and is defined as the one sided green leaf area per unit ground surface area (Chen et al. 1992). LAI is valuable for measuring vegetation density (Watson, 1947), photosynthesis (Wells, 1991), plant productivity (Loomis & Williams, 1963), water use (Richards & Townley-Smith, 1987), and has been applied for biomass estimation and yield predictions in precision agriculture (PA) (Duchemin et al., 2008). Traditional LAI measurements taken by hand are time consuming, costly, and error prone (Li, 2019, Yao 2008). Remote sensing approaches to estimate LAI using multispectral and hyperspectral imagery have been developed and applied at the global and regional scale using satellite and other high atmosphere sensors (Garrigues et al 2008). Use of satellite imagery to estimate within-field variability of LAI for PA applications is of interest, but imagery at this

scale can be limited by atmospheric conditions, spatial resolution, and temporal resolutions (Moran et al. 1997). For example, Landsat 7 and Sentinel 2 have spatial and temporal resolutions of 30 m and 10 m respectively and 16-day and 5-day temporal resolutions respectively. For some PA applications, these spatial and temporal densities may be too limiting.

Unmanned Aerial Vehicles (UAVs) are generally inexpensive, easy to operate, and quickly deployable. UAVs can provide remotely sensed data of entire fields, overcome the limitations of satellite imagery and provide spatial data not feasible from proximal sensors. UAVs in PA can be used for fertilizer estimation, crop yield estimates, weed detection, general management and evapotranspiration estimation (Tsouros et al, 2019). Vegetation indices derived from remotely sensing crop canopies are simple and effective algorithms for quantitative and qualitative evaluations of vegetation cover, vigor and growth dynamics (Xue 2017, Carroll et al. 2017). Both vegetation indices and LAI deal with crop canopy characteristics. Li 2019 and others have established that there is a relationship between vegetation indices and LAI. Because of their versatility and widespread availability, this study focuses on estimating LAI using low-cost consumer grade UAV systems equipped with standard red, green, blue (RGB) digital cameras and lightweight drones for crop growth monitoring. These are affordable systems that offer user-friendly operation and serve as a reliable resource for PA management. RGB orthomosaics made from the UAV images and the UAV point cloud of the crop canopy can further be used to extract RGB values and calculate visible vegetation indices (VVI) and crop surface models for estimating LAI and other growth indicators such as biomass and plant height (Bendig et al. 2015). VVI's have been shown to be a valuable crop monitoring tool as well as an approachable resource for managers considering that no modifications to UAVs are required (Broge & Leblanc 2001, Xue & Su 2017)

Identifying the most useful VVIs to estimate within-field variation of LAI is only part of the approach to remotely estimating LAI. Identifying the optimal spatial resolution as well as the method of acquiring data at that spatial resolution is also important for accurate estimation. Determining the optimal spatial resolution for remote LAI estimation is vital because of the variability that exists within remote imagery of crops. If the spatial resolution is too fine, the results will be noisy and potentially oversensitive to features such as row space, weeds, bare patches, and rock outcroppings. On the other hand if the spatial resolution is too large the spatial variation within field will be smoothed over and lost. Curran et al. (1988) described the complexity of optimal spatial resolution for remote LAI. They showed that spatial resolution between two and five meters was most accurate when estimating within-field variation of LAI. However, not much follow up research has been conducted in recent years with new technological developments – including the use of UAVs. Atkinson (1997) found that the optimal spatial resolution is defined as one that maximizes the information per pixel, and this maximum is realized when the semi variance at a lag of one pixel is maximized. Specifically, the most appropriate spatial resolution for small-scale agricultural mapping of in field spatial variation in the images was between 0.5 m and 3 m.

In addition to determining the optimum spatial resolution at which to sample remote imagery, the method of data resampling is equally important. There are two data resampling methods examined in our research, direct and ladder resampling. Direct resampling takes the native pixel resolution (0.06 m in this study) and resamples the data directly to the desired spatial resolution. The resampling tool samples a small average around a pixel of interest. For the direct resampling method there is potential to lose integrity of the actual spectral reflectance data of the crop canopy because of this pixel averaging. The alternative method of data resampling is the ladder

resampling method. This does the same process as the direct method but over a more gradual jump in spatial resolution. Instead of one averaging of neighboring pixels, there is multiple, thus potentially exhibiting the actual characteristics of the crop canopy.

Our study was conducted based on the working hypothesis that the within-field variability of wheat LAI can be accurately estimated using imagery acquired from a consumer grade UAV. The first objective was to identify the most accurate VVIs to estimate within-field variation of LAI using a consumer-grade UAV. Li et al (2019) found that while VARI was the most appropriate color index for LAI remote estimation, they acknowledged that more research is needed to find the best operation mode, most suitable ground resolution and optimal predictive methods for practical applications. The second research objective was to determine the most suitable spatial resolution for remote estimation of within-field variability of LAI. The final objective is to examine the most accurate resampling method at various spatial resolutions for describing spatial variation of LAI in an irrigated wheat field. It is hypothesized that the most accurate spatial resolution is 2 m generated from native (0.06 m) resolution to a 2 m resolution using Ladder resampling. This is because 2 m resolution removes potential error and bias that could be introduced from aerial anomalies such as missing crop rows, weed patches, and bare soil.

MATERIALS AND METHODS

Site Description

This study was conducted using five data collection events during the 2019 and 2020 growing seasons at two locations, one near Grace, ID and the other near Rexburg, ID. The Grace, ID location (42.60904, -111.788, 1687 m above sea level) is a commercial seed potato (*Solanum*

teberosum L.) and winter wheat production field (22 ha). The soil at the Grace location is a Rexburg-Ririe complex with 1 to 4 percent slopes and a silty-clay-loam texture. Rexburg and Ririe soils are both coarse-silty, mixed, superactive, frigid Calcic Haploxerolls with 5 percent rock outcroppings that derive from alluvial influenced loess. In this field, patches of shallow and emerged bedrock cover a total area of 0.3 ha that are not farmed because of potential equipment damage. Mean annual precipitation is 355 mm with the majority of the precipitation typically falling as snow in the winter and early spring. Average annual temperature is 6.1 C and there are 80-110 frost-free days during the growing season. Irrigation is applied using a 380 m center-pivot sprinkler system equipped with variable rate irrigation technology (Growsmart Precision VRI, Lindsay Zimmatic, Omaha, NE, USA).

The Rexburg, ID location (43.800752, -111.790064, 1518 m above sea level) is a wheat production field within a crop rotation of wheat and alfalfa. The study at this site was conducted on spring wheat (*Triticum Aestivum* L.) grown on 22.7 ha. The soil is a combination of Pocatello Variant silt loam and a Ririe silt loam with 2-8 percent slopes. Pocatello and Ririe soils are coarse-silty, mixed, calcareous, frigid, Typic Xerorthents and coarse-silty, mixed, frigid, Calcic Haploxerolls. The dominant field features are a relatively steep rolling 17 m slope from the southern end to the northern end and shallow soil. Average annual precipitation is 339 mm with the majority of the precipitation falling as snow in the winter and early spring. Average annual temperature is 6.6 C with an 80 to 100 frost free day growing season. Irrigation is applied using a 370 m long center-pivot sprinkler equipped with variable rate irrigation technology (Growsmart Precision VRI, Lindsay Zimmatic, Omaha, NE, USA).

Leaf Area Index Measurements

Leaf area index data were collected with an AccuPAR model LP-80 PAR/LAI Ceptometer at pre-determined geographic points within each field (100 points at Grace and 66 points at Rexburg, Figures 1 & 2)(Kerry et al. 2003). LAI (Chen et al. 1992; Boegh 2002) is defined as the total upper leaf surface area divided by the corresponding land area. The ceptometer calculates LAI based on the above and below canopy photosynthetically active radiation (PAR) measurements along with other variables that relate to the canopy architecture and position of the sun. These variables are the zenith angle, a fractional beam measurement value, and a leaf area distribution parameter (Also known as χ) for a particular canopy. The AccuPAR ceptometer automatically calculates both the zenith angle and fractional beam reading, and requires users to input a value for χ in its setup. At each point, the operator collected a single baseline measurement of the photosynthetically active radiation (PAR) above the canopy. Then, the operator collected PAR measurements below the canopy in each of the four cardinal directions rotating around a single point. The ceptometer then compares the light intensity above and below the canopy and uses the difference in intensity between the two readings to calculate LAI.

UAV Image Acquisition and Processing

A DJI Phantom 4 outfitted with a Sentera single NIR sensor and RGB camera was flown at the fields. The Phantom 4 Pro Camera has a 2.54 cm CMOS with 20 M effective pixels. A 3 axis gimbal integrated with the inertial navigation system stabilized the camera during flight. The UAV's followed automated flight paths created with DroneDeploy (DroneDeploy, 2020) that imaged the entirety of each field at both 91.44 m above ground level (AGL) and 118.87 m

above ground level (AGL) with at least 80% image side and end overlap in the flight paths. Images for Grace were collected May 31, 2019, June 26, 2019 and July 8, 2020, during optimum UAV operating times (11:00 am-2:00 pm). Images for Rexburg were collected May 30, 2019 and June 25, 2019 during optimum UAV operating times (Table 1). The data were processed in Web OpenDroneMap (ODM, 2020). All the individual photos of each field were imported into WebODM and reviewed. The post-processing started with aerial images that are batched together by using the motion of the drone, and a sparse point-cloud of tie points that tie all the images together was created. Next the point cloud was densified into a 3D point cloud. This enabled it to do a surface reconstruction that could be textured. Lastly the textured surface was used to build a mosaicked orthophoto (Van Rees 2017) (Figure 3). WebODM produces an array of file types and for this project we used GeoTIFFs. The GeoTIFFs were exported to be processed in ArcGIS Pro. The RGB images were acquired with a ground resolution of 0.06 m at 91.44 m height and were saved with GPS location information in GeoTIFF format (Figure 10).

Visible Vegetation Index (VVI) Calculations

The visible bands of light have separate and distinct wavelengths from one another. Blue has a wavelength of 450 to 510 nm, green is 530 to 590 nm, and red is 640 to 670 nm. However there exists overlap in reflectance perception in these bands in both human and technological receptors of how these are detected. There is a large percentage of overlap between how the green and red bands are sensed compared to the blue band (Yamaguchi et al. 2008). Visible imagery is made up of combinations of these three bands. Instead of wavelength values, modern computer monitors use red, green, and blue LEDs to produce the full range of colors. Each color band had a digital number value range of 256. Each pixel in the imagery will have a value in red,

green, and blue ranging from 0 to 256 (Montgomery, 2017). Upon completion of image post-processing, digital number values of the red, green, and blue bands (380- 740 nanometers) for each sample point where LAI was measured were extracted from the UAV orthophoto pixels associated with each location. RGB band values can quantitatively measure the radiance and reflectance characteristics in visible spectrum of crop canopy (Hansen et al. 2003, Hunt et al. 2013). Equations 1-3 represent how RGB band values are calculated. Table 2 shows the 12 VVIs that were calculated and evaluated in this research. These digital pixel values were used to calculate VVI values at the sample points where LAI was taken in the field with the objective of finding a VVI that is highly correlated with LAI that can be used to measure LAI remotely.

$$R=R/(R+G+B) \quad \text{Equation 1.}$$

$$G=G/(R+G+B) \quad \text{Equation 2.}$$

$$B=B/(R+G+B) \quad \text{Equation 3.}$$

Regression Modeling

Linear regression analysis was conducted between measured wheat LAI and each VVI at all spatial resolutions, resampling methods, and sampling dates. Linear models are simple and are therefore widely applicable for a variety of uses. The predictive performance of each single variable was evaluated and compared based on the linear regression models for wheat LAI estimation. The linear regression models were built using equation 4,

$$LAI=bX+a, \quad \text{Equation 4.}$$

Where LAI represents the wheat leaf area index, X represents the single input predictor variable, b and a represent the slope and intercept of the fitted line of the LR model, respectively.

Resampling Methods and Spatial Resolutions

The DJI Phantom 4 camera has a native spatial resolution of 0.06 m at 91.4 m above ground level. Such fine resolutions may be inappropriate in remote estimation of LAI and other canopy metrics (Atkinson, 1997), and previous research has shown that spatial resolutions ranging between 0.5 to 5 m are more accurate (Atkinson, 1997; Curran, 1987) for LAI estimation and mapping. UAV imagery is not typically acquired at this coarser resolution. Using native resolution can introduce unwanted artifacts from the observed field such as missing rows of crops, weed patches, and border areas. This can make it overall more difficult to apply remote sensing to PA.

In our research there are two methods that are used, direct and ladder resampling. In the direct resampling method we resampled the native image directly from native resolution to the desired spatial resolution in ArcGIS Pro. For the ladder resampling method we gradually resampled the native imagery up to the optimal resolution through 0.25 m, 0.25 m resized into 0.5 m, 0.5 m resized to 1 m, 1 m resized to 2 m, 2m resized to 3m (Figure 4).

Resampling was done in ArcGIS Pro (ESRI, ArcGIS desktop: Release 10, Redlands, CA, USA) by uploading the native orthomosaics of the observed fields and running them through both direct and ladder resampling methods. After imagery of all desired spatial resolutions, 0.1 m through 3.0 m, digital number RGB values were extracted from the resized pixel containing the pre-determined ground sample points within each field (Figures 1 & 2) and the RGB values were used to calculate VVIs which were compared to hand measured field LAI values using linear regressions.

Statistical Analysis

Samples from all dates (n= 382) were split into training and test data sets by date and then combined into a comprehensive data set. The data for each sampling date was split into 2/3 for training and 1/3 for testing. The comprehensive training data had 249 points and the comprehensive testing data had 133 points. Coefficient of determination (R^2) values were calculated on the training data between the VVIs and LAI values. Root mean square error (RMSE) were calculated to indicate the training model results. Linear regression models were established for each VVI. The correlations between wheat LAIs and each VVI at each spatial resolution and resampling method were analyzed based on the performance of the LR models. The accuracies of these regression models were assessed using the test data samples by measuring the root mean square error (RMSE) and mean absolute error (MAE) Equation (Equation 9) between the predicted LAIs and the observed LAIs. Root mean square error is the standard deviation of the residuals or prediction errors. RMSE is a measure of how spread out the residuals are or how concentrated the data is around the best fit line. Absolute error is the amount of error in the measurements. It is the difference between the measured value and the predicted value. The mean absolute error is the average of all the absolute errors. Both RMSE and MAE indicate the average prediction error. The statistical analysis was performed using R software (v.3.6.1, R Development Core Team, 2020) and Microsoft Excel.

RESULTS

Variability of Wheat Leaf Area Index

Wheat LAI values varied greatly as expected with sampling times ranging across three months of the growing season. LAI values increased as the growing season progressed. The LAI

values across all sampling times and both locations ranged from 0.10 to 5.45 in the training data set and 0.13 to 5.96 in the test data set (Table 3). These ranges compare well with other reported wheat LAI values (Nielsen et al. 2012).

Evaluation of Visible Vegetation Indices, Resolution, and Resampling Methods

Twelve different VVIs were evaluated in our study to determine the relationship of each VVI with measured LAI with the objective to determine the VVIs that would be able to estimate LAI most accurately based on a simple linear regression. The regressions were made using pooled data from all five sampling events. The twelve VVIs that were evaluated varied widely in which visible color bands were used and how the equations were formulated (Table 2). The strength of the linear regression models were statistically evaluated by comparing the coefficient of determination values (R^2 , Figure 5), RMSE (Figure 6), and MAE (Figure 7). The NGRDI and MGRVI exhibited the best correlation with wheat LAI ($R^2=0.66$, RMSE= 0.73).

Temporal Variation in Remote Sensing and Modeling Accuracy for Wheat Leaf Area Index

LAI and UAV sampling occurred across the wheat growing season from May to July, representing a large portion of the growing season. Figures 5 and 6 show the R^2 and RMSE results for the Grace 3 meter direct and ladder VVI models. The 3 meter spatial resolution consistently had the best LAI predictive model results (VARI RMSE=0.74) when compared to the other spatial resolutions, so this resolution is used to illustrate the temporal variation. The RMSE results for the May sampling for all 12 VVI models lie within the 0.2 to 0.4 range while the RMSE results for both the later samplings (post canopy closure) range between 0.74 and 1.24. VARI at Grace in May 2019 has an RMSE of 0.29 but in June and July respectively the RMSE values are 0.8 and

0.77 (Figure 6). Likewise NGRDI and MGRVI had RMSE values in Grace during May 2019 of 0.3 but in June and July they are 0.86 and 0.76 respectively.

DISCUSSION

Visible Vegetation Index Comprehensive Performance for Wheat Leaf Area Index Estimation

Twelve commonly used VVIs were selected to test the ability to use UAV imagery for assessing within-field variation of LAI. The results (Table 4.) showed that the visible atmospherically resistant index (VARI), normalized green-red difference index (NGRDI), and modified green-red vegetation index (MGRVI) had the best performance compared to the other VVIs in both training ($R^2= 0.66, 0.66, 0.66$) and test datasets (RMSE=0.74, 0.73, 0.73; MAE=0.57, 0.56, 0.56). This result supports other findings where these three VVI showed excellent feasibilities for barley and grass biomass estimation (Kaivosoja et al) and rice yield prediction (Zhou et al). These three VVI LR models for predicting LAI in irrigated wheat have simple structures that are convenient for technical implementation and practical in field applications. Some VVIs showed little to no use for LAI prediction modeling. ExB, WI, IKAW, RGBVI and VEG all had poor RMSE values when compared to VARI, NGRDI, and MGRVI. The characteristic that sets these indices apart from the successful LAI estimation indices is that they tend to have the blue band as a heavily weighted component in the equation. For example the excess blue index is $1.4*b-g$. The red band is omitted entirely and then the green band is subtracted from the multiplied blue band. This suggests that the blue band is much less useful in remote estimation of LAI. Both NGRDI and MGRVI totally omit the blue band. VARI does include the blue band in a sense, $(g-r)/(2g+r-b)$, however the inclusion of the blue band in the equation is only to subtract it from the total combination, isolating the red and green band

combinations. While these indices may be useful for other remote sensing applications, they held little value for LAI estimation in our study. Across all sampling dates, spatial resolutions, and resampling methods these VARI, NGRDI, and MGRVI outperformed the others. However, the RMSE is more sensitive to large errors due to its quadratic scoring rule, while the MAE measures the absolute differences between prediction and actual observation. A good example of these large errors may be in Grace where there are occasional islands of volcanic rock within the field that affect the growth of the crop around them. If digital number values are taken in those areas they may shift significantly the results of the RMSE.

Spatial Resolution Results

VARI, NGRDI, and MGRVI through direct resampling had lower RMSE and MAE values at 1 and 3 m spatial resolutions (Figure 6 & 7) with RMSE values ranging from 0.75-0.78. Those VVIs were also found acceptable at 1, 2, and 3 meter spatial resolutions through the ladder resampling (figures 3b, 4b, 5) with RMSE values of 0.73 to 0.76. The spatial resolution results show that UAV imagery with finer resolutions optimally should be resampled to a courser spatial resolution when estimating LAI. Curran et al found that spatial resolution between 2 and 5 meters was most accurate when estimating field LAI. The most accurately performing models came from those at 3 meter spatial resolution (Table 4). These results are in line with the results that previous research has found. Further research could also be done into the effectiveness of UAVs when compared to satellite imagery.

Resampling Method Differences

With the variety of GIS programs and technology, establishing a methodology of resampling or resizing UAV imagery to the desired spatial resolution is vital. In this research there are two methods that are examined, direct and ladder resampling. Direct resampling is resampling the native image directly from native resolution to the desired spatial resolution in a program like ArcGIS Pro. However, this may produce different and potentially less accurate measurements than the other form of resampling. Ladder resampling is done by gradually resampling the native imagery up to the optimal resolution through a series of finer resolutions. For example, native resized to 0.25 m, 0.25 m resized into 0.5 m, 0.5 m resized to 1 m, 1 m resized to 2 m, etc (Figure 4).

When examining the highest accuracy predictive models for LAI estimation there appear to be differences between the direct and ladder resampling methods. The ladder produced an overall lower RMSE value than the direct method. At the 3 meter spatial resolution VARI direct has an RMSE of 0.78 but with the ladder resampling method it becomes 0.74. Both NGRDI and MGRVI direct had RMSE values of 0.78 for direct resampling or 0.73 with ladder resampling. All these models are within acceptable ranges but the ladder resampling method performs more accurately. Figure 8 examines the differences of the ladder and direct resampling methods across spatial resolutions for the top VVI models. The direct methods results in a loss of predictive power, especially at models in the 0.25, 0.5 and 2 meter resolutions. The ladder resampling (Figure 6) has a smoothing effect on the RMSE values as the spatial resolution increase. The ladder resampling method is more representative of the actual reflectance values of the crop canopy. This is due to the gradual pulling in of pixel values around the pixel of interest rather than going directly from a small pixel size to a larger pixel size. The additional post processing

of the pixels of interest will bring more strength into the dataset. From native to 3 meters the RMSE values gradually decrease until they reach the lowest values of 0.73. The direct resampling method produces jagged and varied RMSE values from the models as they increase in spatial size. Even though the difference in LAI model accuracy may be slight it may be beneficial to resample UAV imagery through the ladder method especially when coarser spatial resolutions are desired. It seems there is a loss of pixel integrity if a native 6 cm pixel is resampled directly to larger spatial resolutions, especially at the 2 meter resolution.

Temporal Remote Sensing Variation

Figures 9 and 10 represents how RMSE model and R^2 values in Grace ID change as the growing season of wheat progresses. In all variables, remotely sensed LAI models were able to better predict LAI in May than in June or July. UAV imagery for remote estimation of LAI performs more accurately at the beginning of the wheat growing season. The crop canopy has not yet closed and plant spatial variation is easily detectable. Figure 9, 10, 11, 12 demonstrates that remotely sensed LAI models are less accurate later in the growing season

The temporal variation in model accuracy suggests that managers need to acquire UAV imagery early on in the season before wheat canopy closure for best LAI model estimation results (Figures 9, 10). These trends are mirrored in the results for Rexburg May 2019 and June 2019 in Figures 11 & 12. VARI Direct in Rexburg in May 2019 has an RMSE of 0.16 and in June 2019 an RMSE of 0.51 in June 2019.

The results could indicate that applying remote sensing at the beginning of the growing season prior to wheat canopy closure would provide the most benefit for identifying plant trends and precision agriculture management zones.

CONCLUSION

This study showed the potential of using visible vegetation indices derived from UAV imagery from consumer grade UAVs to estimate wheat LAI based on field measurements and linear regression predictive modeling results. VARI, NGRDI, and MGRVI showed acceptable performance in VVI based linear regression models. The ladder data resampling method was more accurate than direct resampling for native UAV imagery to coarser spatial resolutions. A spatial resolution of 3 m performed the highest when compared to less coarse resolutions. VARI, NGRDI, and MGRVI at 3 m spatial resolution through the ladder resampling had the best ability to predict LAI in wheat. The linear regression models all performed more accurately in May prior to canopy closure rather than in June or July. Future research is needed to compare UAV and satellite imagery and explore the cost benefit analysis of UAVs. Additionally, the most accurate methodology for LAI remote estimation such as optimum flight height, UAV selection, and a determination of when LAI needs to be estimated for the most accurate precision agriculture maps needs to be explored in the future. Future research should examine the potential this has for ET estimation derived from remotely estimated LAI.

LITERATURE CITED

- Atkinson, P. M. (1997). Selecting the spatial resolution of airborne MSS imagery for small-scale agricultural mapping. *International Journal of Remote Sensing*, 18(9), 1903–1917.
<https://doi.org/10.1080/014311697217945>
- Bendig, J., Yu, K., Aasen, H., Bolten, A., Bennertz, S., Broscheit, J., Gnyp, M. L., & Bareth, G. (2015). Combining UAV-based plant height from crop surface models, visible, and near infrared vegetation indices for biomass monitoring in barley. *International Journal of Applied Earth Observation and Geoinformation*, 39, 79–87. <https://doi.org/10.1016/j.jag.2015.02.012>
- Broge, N. H., & Leblanc, E. (2001). Comparing prediction power and stability of broadband and hyperspectral vegetation indices for estimation of green leaf area index and canopy chlorophyll density. *Remote Sensing of Environment*, 76(2), 156–172. [https://doi.org/10.1016/s0034-4257\(00\)00197-8](https://doi.org/10.1016/s0034-4257(00)00197-8)
- Boegh, E., H. Soegaard, N. Broge, C. Hasager, N. Jensen, K. Schelde, and A. Thomsen. "Airborne Multi-spectral Data for Quantifying Leaf Area Index, Nitrogen Concentration and Photosynthetic Efficiency in Agriculture." *Remote Sensing of Environment* 81, no. 2-3 (2002): 179-193.
- Carroll, D. A., Hansen, N. C., Hopkins, B. G., & Dejonge, K. C. (2017). Leaf temperature of maize and Crop Water Stress Index with variable irrigation and nitrogen supply. *Irrigation Science*, 35(6), 549–560. doi: 10.1007/s00271-017-0558-4
- Chen, J. M., & Black, T. A. (1992). Defining leaf area index for non-flat leaves. *Plant, Cell and Environment*, 15(4), 421–429. <https://doi.org/10.1111/j.1365-3040.1992.tb00992.x>

- Curran†, P. J., & Dawn Williamson‡, H. (1988). Selecting a spatial resolution for estimation of per-field green leaf area index. *International Journal of Remote Sensing*, 9(7), 1243–1250.
<https://doi.org/10.1080/01431168808954931>
- DeJonge, K.C., A.L. Kaleita, and K.R. Thorp. 2007. Simulating the effects of spatially variable irrigation on corn yields, costs, and revenue in Iowa. *Agricultural Water Management* 92: 99-109.
- Duchemin, B., Maisongrande, P., Boulet, G., & Benhadj, I. (2008). A simple algorithm for yield estimates: Evaluation for semi-arid irrigated winter wheat monitored with green leaf area index. *Environmental Modelling & Software*, 23(7), 876–892.
<https://doi.org/10.1016/j.envsoft.2007.10.003>
- Garrigues, S., Lacaze, R., Baret, F., Morissette, J. T., Weiss, M., Nickeson, J. E., Fernandes, R., Plummer, S., Shabanov, N. V., Myneni, R. B., Knyazikhin, Y., & Yang, W. (2008). Validation and intercomparison of global Leaf Area Index products derived from remote sensing data. *Journal of Geophysical Research: Biogeosciences*, 113(G2).
<https://doi.org/10.1029/2007jg000635>
- Gitelson, A. A., †, Y. G., & Merzlyak, M. N. (2003). Relationships between leaf chlorophyll content and spectral reflectance and algorithms for non-destructive chlorophyll assessment in higher plant leaves. *Journal of Plant Physiology*, 160(3), 271–282. doi: 10.1078/0176-1617-00887
- Hague, T., Tillett, N. D., & Wheeler, H. (2006). Automated crop and weed monitoring in widely spaced cereals. *Precision Agriculture*, 7(1), 21-32.
- Hansen, P. M., & Schjoerring, J. K. (2003). Reflectance measurement of canopy biomass and nitrogen status in wheat crops using normalized difference vegetation indices and partial least squares

regression. *Remote Sensing of Environment*, 86(4), 542–553. [https://doi.org/10.1016/s0034-4257\(03\)00131-7](https://doi.org/10.1016/s0034-4257(03)00131-7)

Hopkins A. P. and Hansen N. C. 2021. Remote Sensing and Spatial Variability of Leaf Area Index Within Irrigated Wheat Fields. This Thesis

Hunt, E. R., Doraiswamy, P. C., McMurtrey, J. E., Daughtry, C. S. T., Perry, E. M., & Akhmedov, B. (2013). A visible band index for remote sensing leaf chlorophyll content at the canopy scale. *International Journal of Applied Earth Observation and Geoinformation*, 21, 103–112. <https://doi.org/10.1016/j.jag.2012.07.020>

Johnson, L. F., & Trout, T. J. (2012). Satellite NDVI Assisted Monitoring of Vegetable Crop Evapotranspiration in California's San Joaquin Valley. *Remote Sensing*, 4(2), 439–455. doi: 10.3390/rs4020439

Kawashima, S., & Nakatani, M. (1998). An algorithm for estimating chlorophyll content in leaves using a video camera. *Annals of Botany*, 81(1), 49-54.

Kerry, R. and M. Oliver. 2003. Variograms of ancillary data to aid sampling for soil surveys. *Precision Agriculture* 4: 261-278.

Li, S., Yuan, F., Ata-Ui-Karim, S. T., Zheng, H., Cheng, T., Liu, X., ... Cao, Q. (2019). Combining Color Indices and Textures of UAV-Based Digital Imagery for Rice LAI Estimation. *Remote Sensing*, 11(15), 1763. doi: 10.3390/rs11151763

Longchamps, L., R. Khosla, R. Reich, and D.W. Gui. 2015. Spatial and Temporal Variability of Soil Water Content in Leveled Fields. *Soil Science Society of America Journal* 79: 1446-1454

Loomis, R. S., & Williams, W. A. (1963). Maximum Crop Productivity: An Estimate 1. *Crop Science*, 3(1), 67–72. <https://doi.org/10.2135/cropsci1963.0011183x000300010021x>

- Louhaichi, M., Borman, M. M., & Johnson, D. E. (2001). Spatially Located Platform and Aerial Photography for Documentation of Grazing Impacts on Wheat. *Geocarto International*, 16(1), 65–70. doi: 10.1080/10106040108542184
- Manuals. (n.d.). Retrieved from <https://www.manualslib.com/products/Decagon-Devices-Accupar-Lp-80-8749930.html>
- Mao, W., Wang, Y., & Wang, Y. (2003). Real-time detection of between-row weeds using machine vision. In *2003 ASAE Annual Meeting* (p. 1). American Society of Agricultural and Biological Engineers.
- Meyer, G. E., & Neto, J. C. (2008). Verification of color vegetation indices for automated crop imaging applications. *Computers and electronics in agriculture*, 63(2), 282-293.
- Montgomery, M. (2019). Image Bands.
https://gsp.humboldt.edu/OLM/Courses/GSP_216_Online/lesson3-1/bands.html.
- Moran, M. S., Inoue, Y., & Barnes, E. M. (1997). Opportunities and limitations for image-based remote sensing in precision crop management. *Remote Sensing of Environment*, 61(3), 319–346.
[https://doi.org/10.1016/s0034-4257\(97\)00045-x](https://doi.org/10.1016/s0034-4257(97)00045-x)
- Nielsen, D. C., Miceli-Garcia, J. J., & Lyon, D. J. (2012). Canopy Cover and Leaf Area Index Relationships for Wheat, Triticale, and Corn. *Agronomy Journal*, 104(6), 1569–1573.
<https://doi.org/10.2134/agronj2012.0107n>
- Neto, J. C. (2004). A combined statistical-soft computing approach for classification and mapping weed species in minimum-tillage systems. *The University of Nebraska-Lincoln*.
- Richards, R. A., & Townley-Smith, T. F. (1987). Variation in leaf area development and its effect on water use, yield and harvest index of droughted wheat. *Australian Journal of Agricultural Research*, 38(6), 983. <https://doi.org/10.1071/ar9870983>

- Trout, T. J., Johnson, L. F., & Gartung, J. (2008). Remote Sensing of Canopy Cover in Horticultural Crops. *HortScience*, 43(2), 333–337. doi: 10.21273/hortsci.43.2.333
- Tsouros, D. C., Bibi, S., & Sarigiannidis, P. G. (2019). A Review on UAV-Based Applications for Precision Agriculture. *Information*, 10(11), 349. <https://doi.org/10.3390/info10110349>
- Tucker, C. J. (1979). Red and photographic infrared linear combinations for monitoring vegetation. *Remote Sensing of Environment*, 8(2), 127–150. doi: 10.1016/0034-4257(79)90013-0
- Watson, D. J. (1947). Comparative Physiological Studies on the Growth of Field Crops: II. The Effect of Varying Nutrient Supply on Net Assimilation Rate and Leaf Area. *Annals of Botany*, 11(4), 375–407. <https://doi.org/10.1093/oxfordjournals.aob.a083165>
- Webster, R. and Oliver, M.A. 2001. Geostatistics for Environmental Scientists (John Wiley and Sons Ltd., Chichester, England)
- Wells, R. (1991). Soybean Growth Response to Plant Density: Relationships among Canopy Photosynthesis, Leaf Area, and Light Interception. *Crop Science*, 31(3), 755–761. <https://doi.org/10.2135/cropsci1991.0011183x003100030044x>
- Woebbecke, D. M., Meyer, G. E., Von Bargaen, K., & Mortensen, D. A. (1995). Color indices for weed identification under various soil, residue, and lighting conditions. *Transactions of the ASAE*, 38(1), 259-269.
- Van Rees, E. (2017, December 22). *OpenDroneMap: a Toolkit for Processing Aerial Drone Imagery*. Commercial UAV News. <https://www.commercialuavnews.com/infrastructure/opendronemap-toolkit-processing-aerial-drone-imagery>.
- Xue, J., & Su, B. (2017). Significant Remote Sensing Vegetation Indices: A Review of Developments and Applications. *Journal of Sensors*, 2017, 1–17. <https://doi.org/10.1155/2017/1353691>

- Yamaguchi, M., Haneishi, H., & Ohyama, N. (2008). Beyond Red–Green–Blue (RGB): Spectrum-Based Color Imaging Technology. *Journal of Imaging Science and Technology*, 52(1), 010201. [https://doi.org/10.2352/j.imagingsci.technol.\(2008\)52:1\(010201\)](https://doi.org/10.2352/j.imagingsci.technol.(2008)52:1(010201))
- Yao, Y., LIU, Q., LIU, Q., & LI, X. (2008). LAI retrieval and uncertainty evaluations for typical row-planted crops at different growth stages. *Remote Sensing of Environment*, 112(1), 94–106. <https://doi.org/10.1016/j.rse.2006.09.037>

FIGURES



Figure 1-1 Leaf area index sample point locations in Rexburg, Idaho irrigated wheat field.

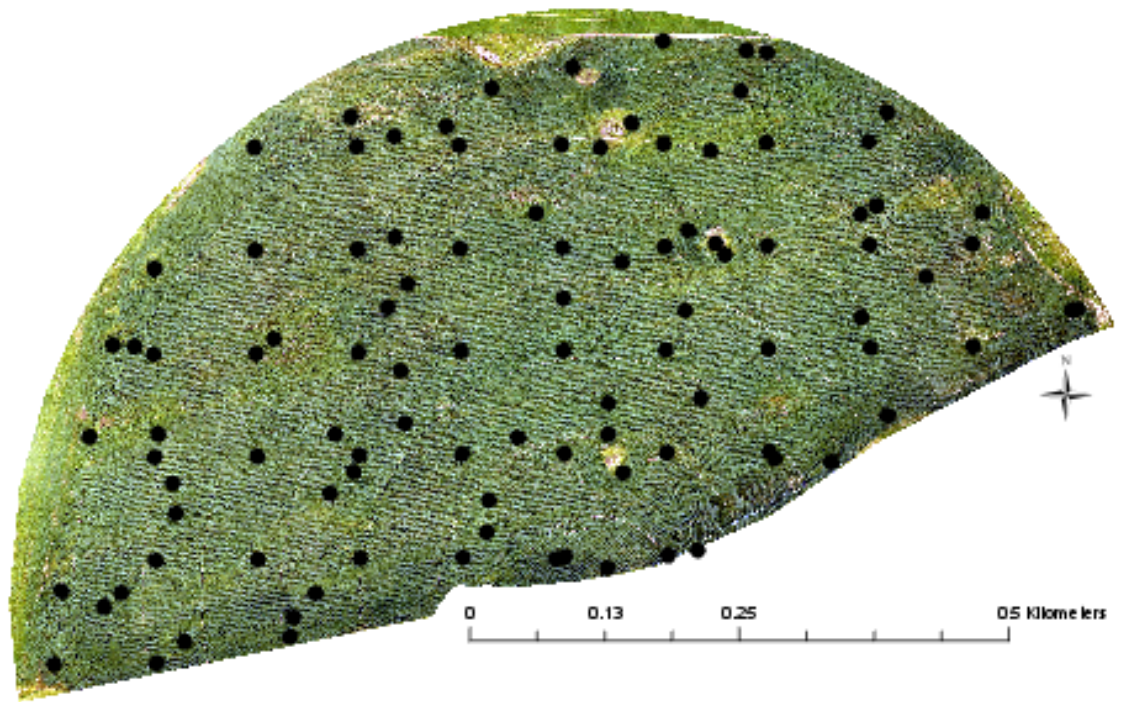


Figure 1-2 Leaf area index sample point locations in Grace, Idaho irrigated wheat field.

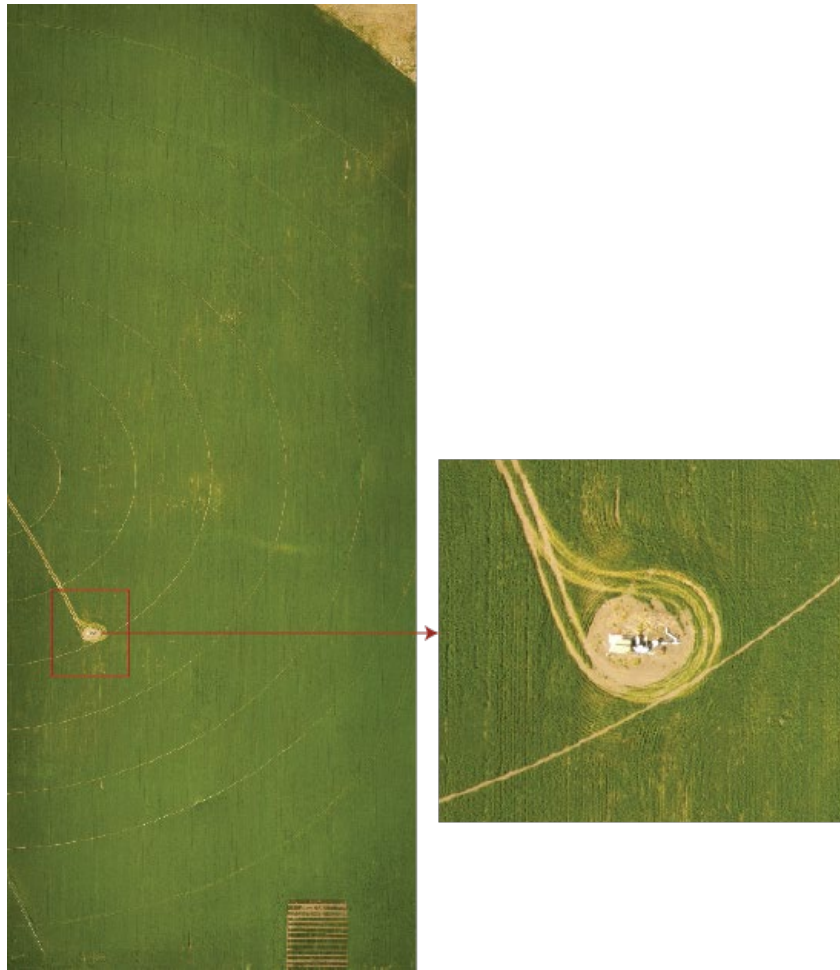


Figure 1-3 Traditional RGB orthophoto generated from images acquired over the Rexburg, ID winter wheat study location on 25 June 2019. The images were acquired with a DJI Phantom 4 flying 300 feet above ground level and processed with Web OpenDroneMap.

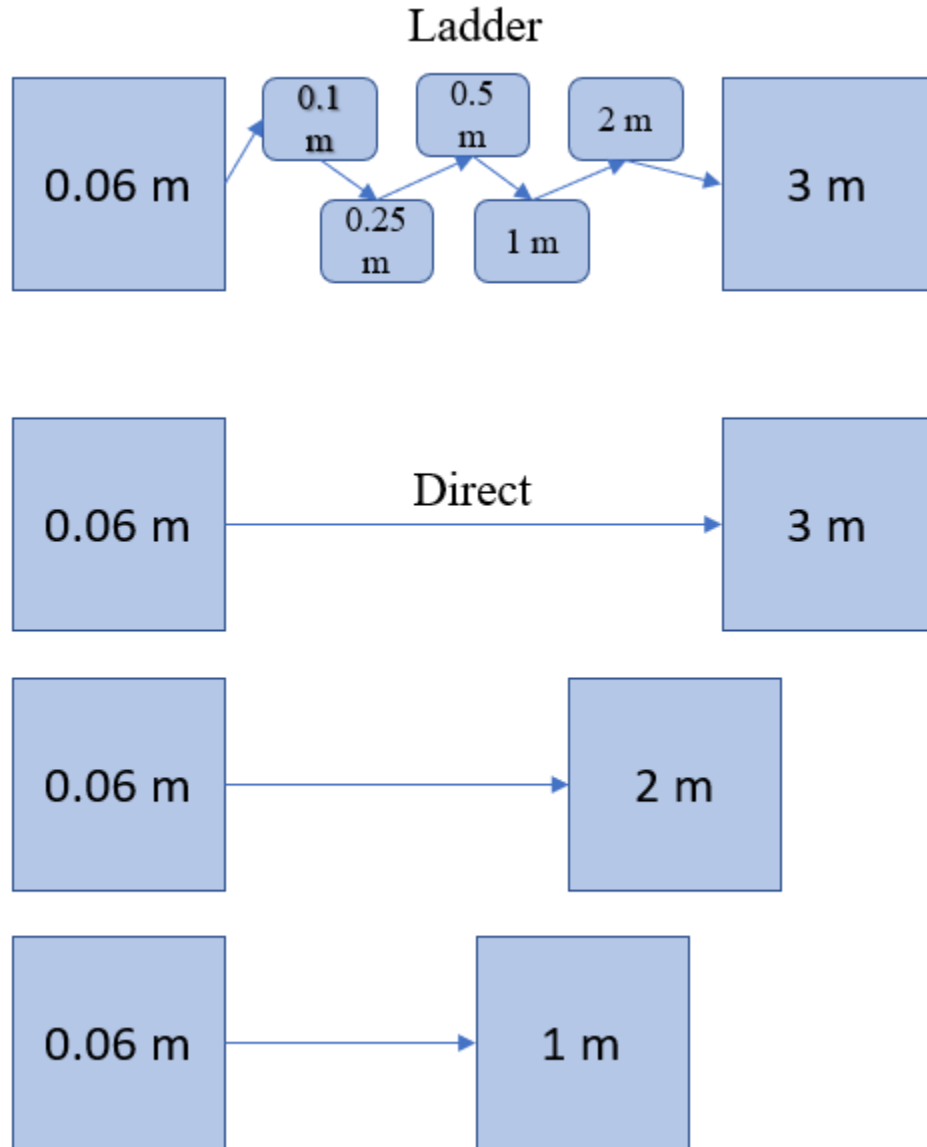


Figure 1-4 Model depicting the ladder and direct resampling method. Direct resampling takes an image in the native resolution and resizes it directly to the desired resolution. Ladder resampling takes an image in the native resolution and resizes gradually through coarser resolutions.

R Squared Statistic of VVIs by Resampling Methodology

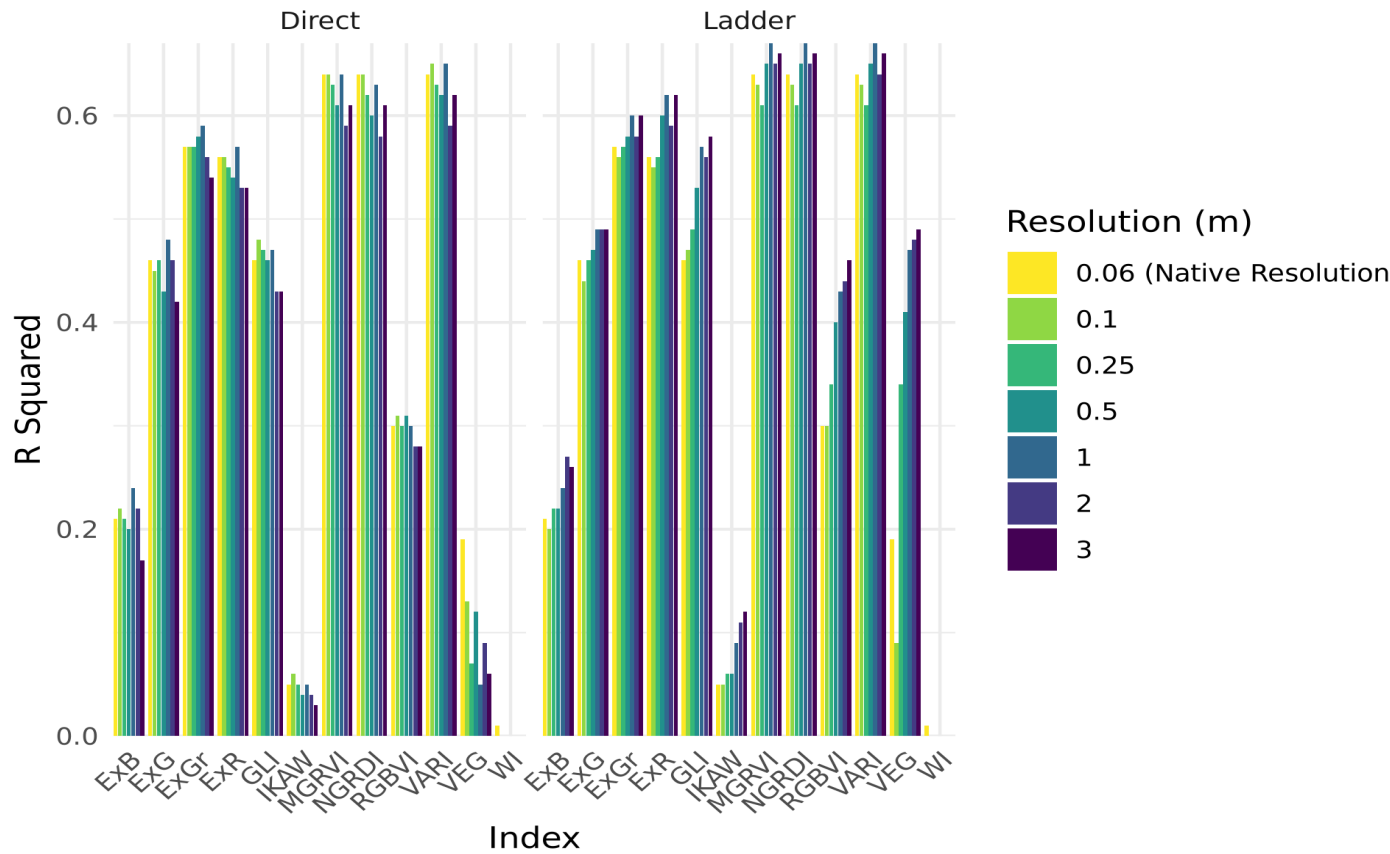


Figure 1-5 Coefficient of determination (R²) values for the correlations of 12 visible vegetation indices (VVIs) with pooled data of measured wheat leaf area index over five sampling events.

Comprehensive RMSE of VVIs by Resampling Methodology

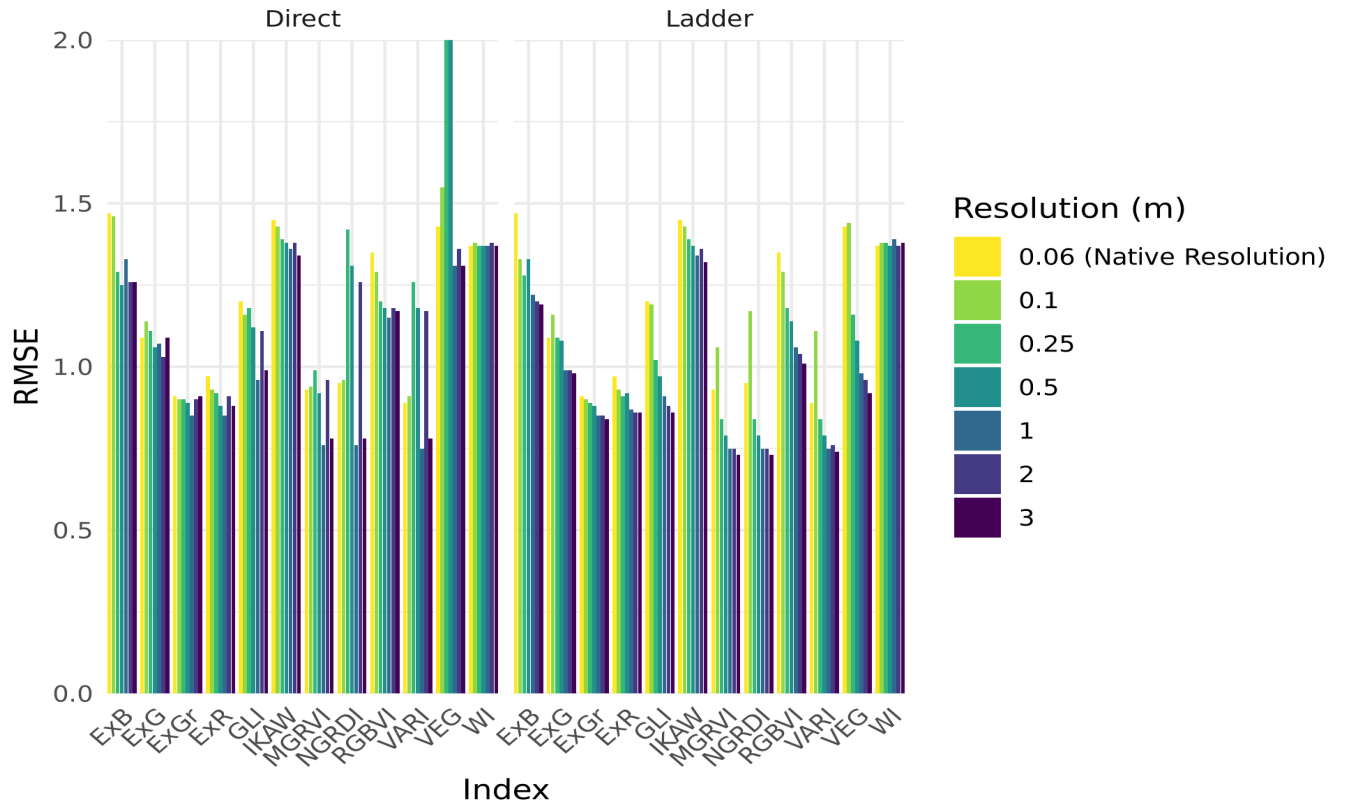


Figure 1-6 Root Mean Square Error (RMSE) values from simple linear regression models of 12 visible vegetation indices (VVIs) with pooled data of measured wheat leaf area index over five sampling events.

Comprehensive MAE of VVIs by Resampling Methodology

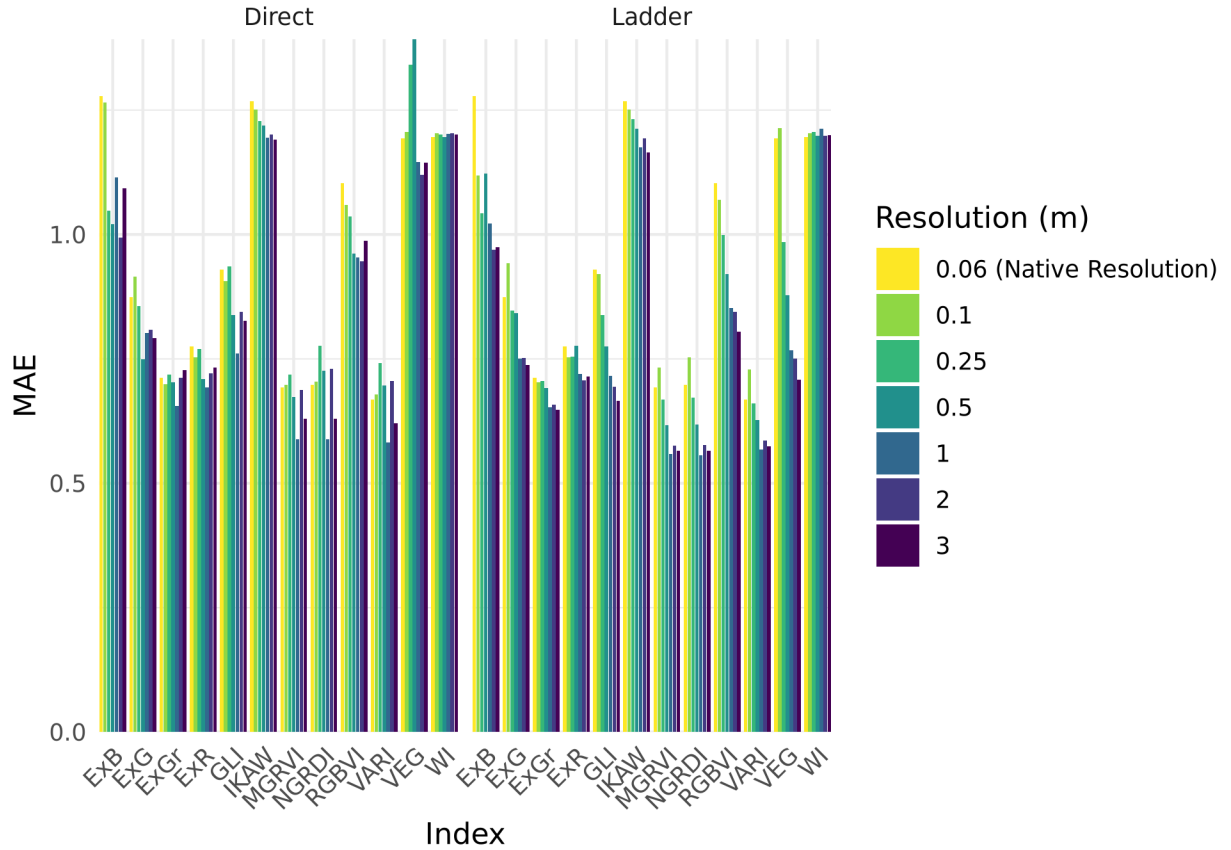


Figure 1-7 Mean Absolute Error (MAE) values from simple linear regression models of 12 visible vegetation indices (VVIs) with pooled data of measured wheat leaf area index over five sampling events.

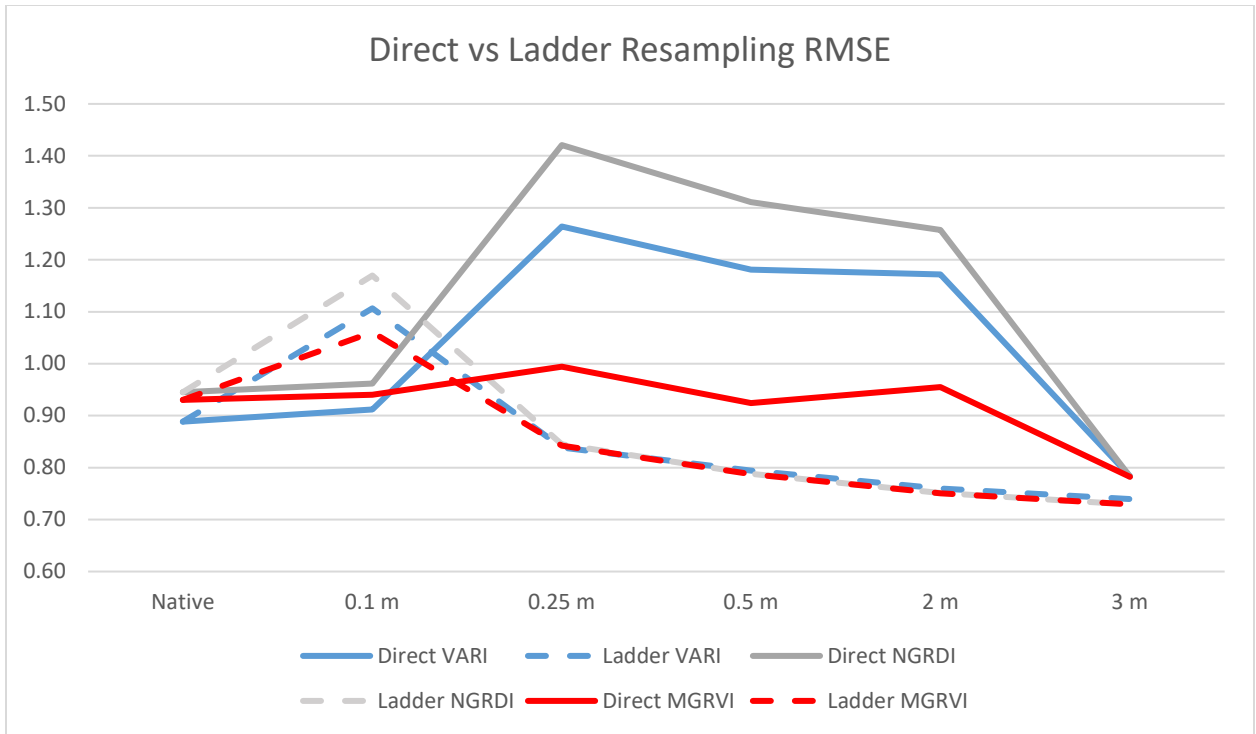


Figure 1-8 Results of the comparison of direct v Ladder resampling methods for VARI, NGRDI, and MGRVI at all spatial resolutions. This shows the variation in RMSE values for each model between the two resampling method.

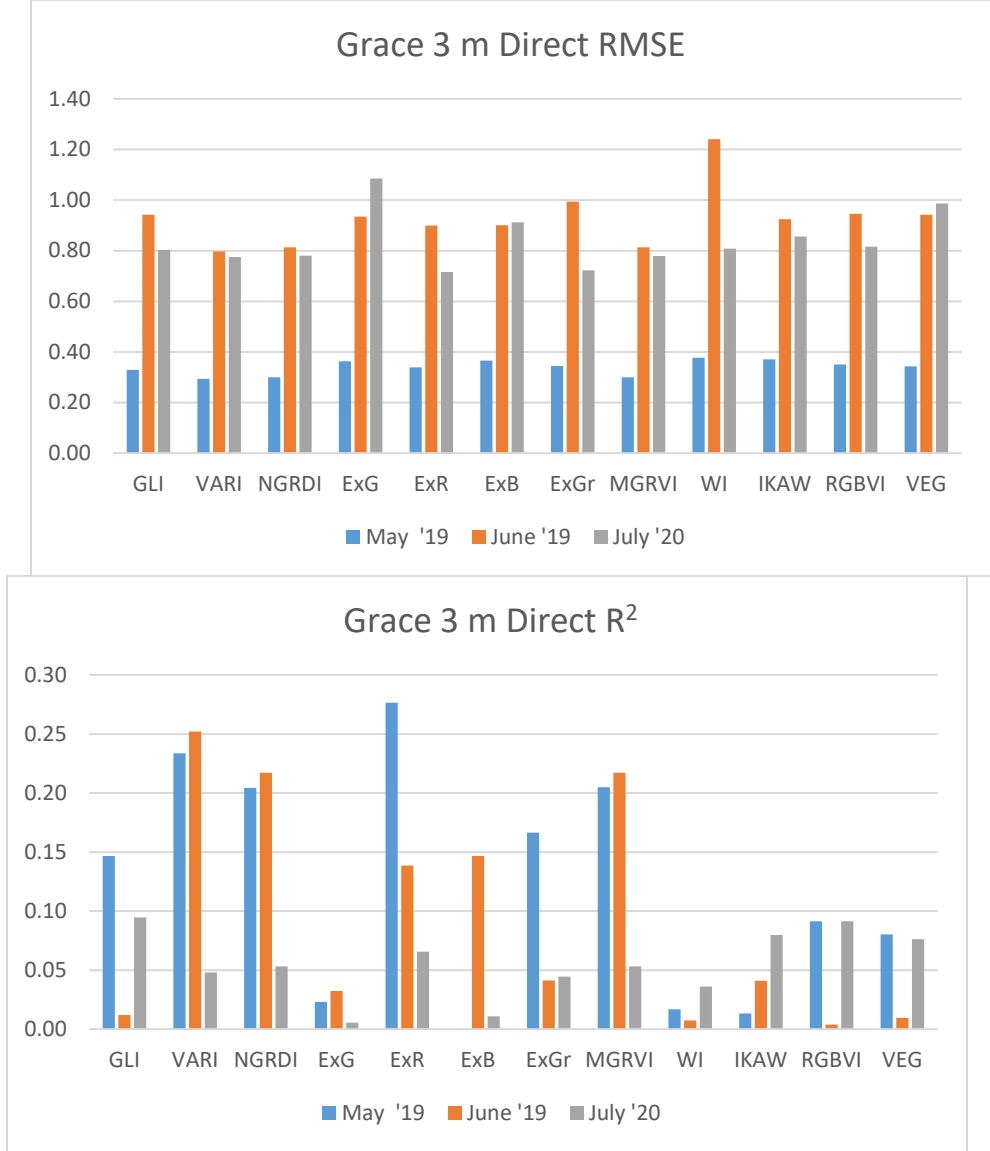


Figure 1-9 (a) Root mean square error values (RMSE) of the VVI- based simple linear regression models for wheat LAI estimation in May 2019, June 2019, and July 2020 in Grace Idaho at 1 meter spatial resolution derived with the Direct resampling method and (b) R2 values between VVIs and LAI.

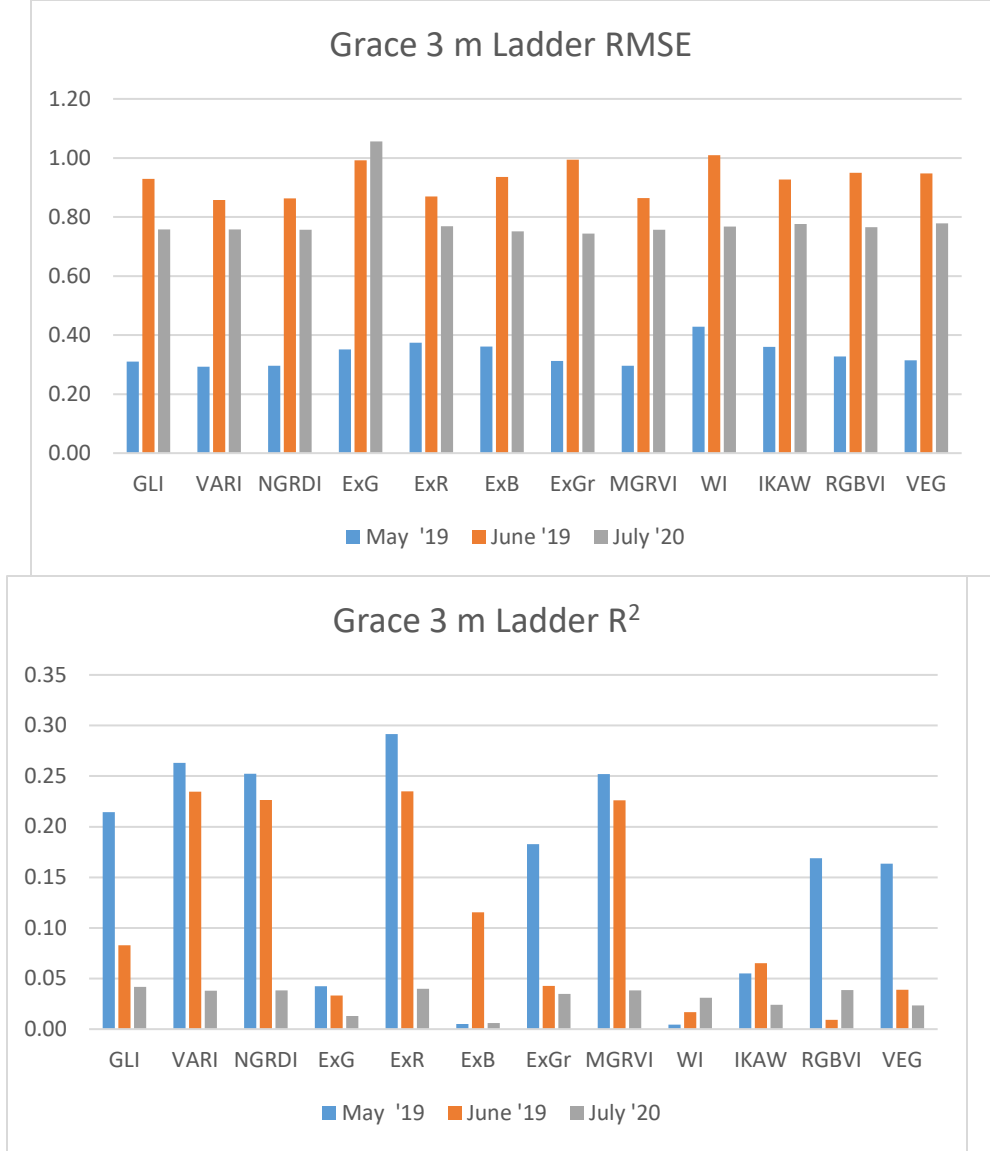


Figure 1-10 (a) Root mean square error values (RMSE) of the VVI- based simple linear regression models for wheat LAI estimation in May 2019, June 2019, and July 2020 in Grace Idaho at 1 meter spatial resolution derived with the Ladder resampling method and (b) R² values between VVIs and wheat LAI.

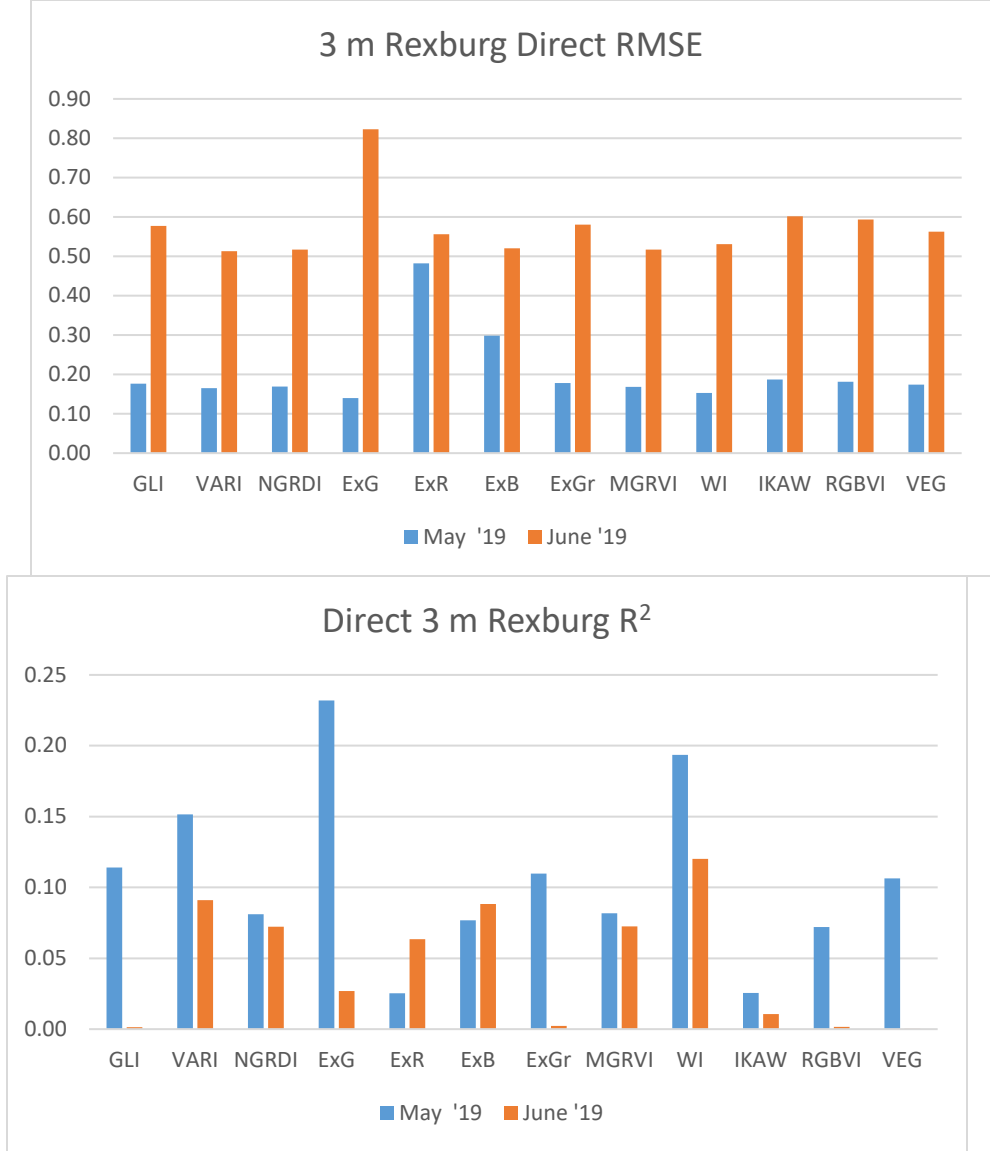


Figure 1-11 (a) Root mean square error values (RMSE) of the VVI- based simple linear regression models for wheat LAI estimation across sampling dates, May 2019, and June 2019 in Rexburg Idaho at 3 meter spatial resolution derived with the Direct resampling method and (b) R² values between VVIs and wheat LAI.

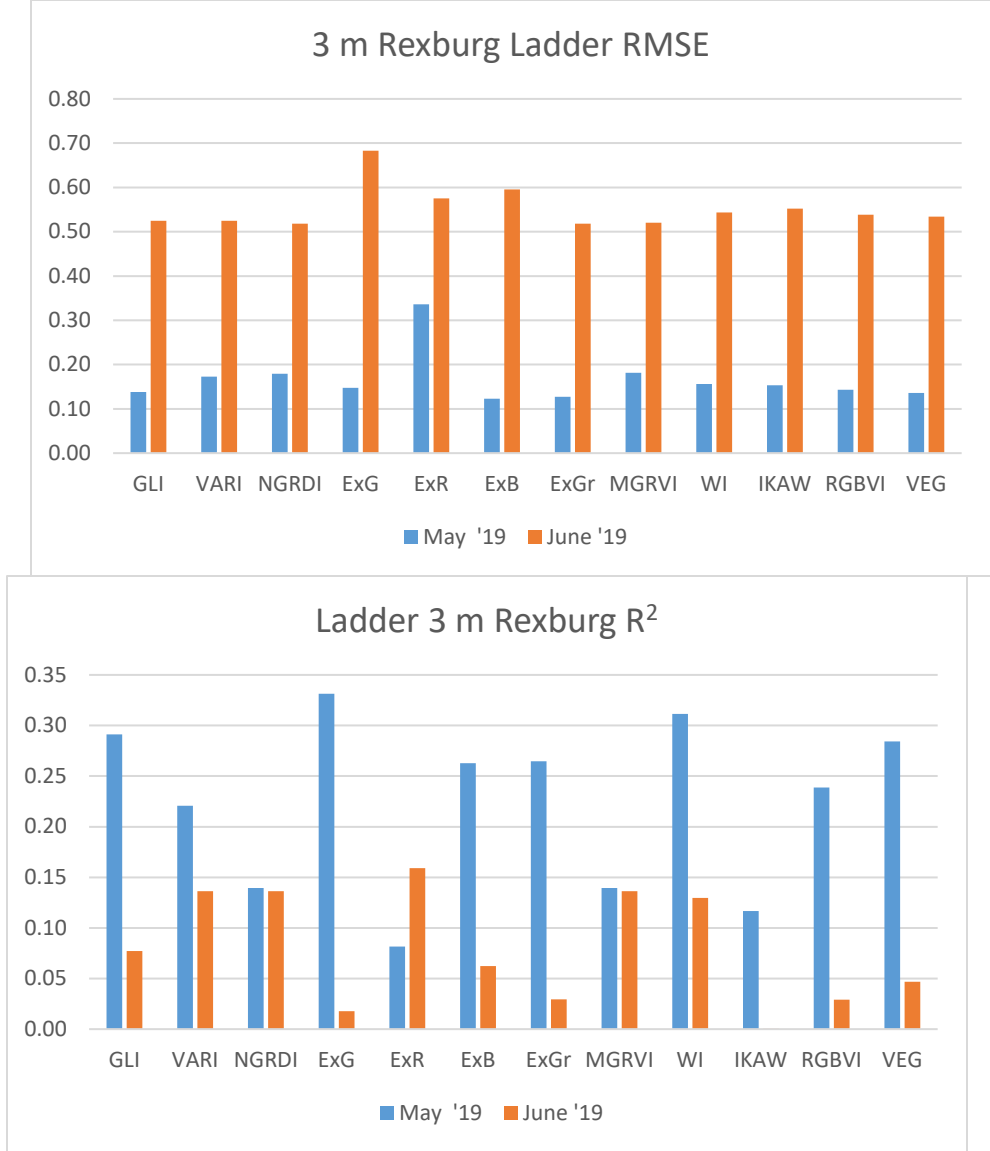


Figure 1-12 (a) Root mean square error values (RMSE) of the VVI- based simple linear regression models for wheat LAI estimation across sampling dates, May 2019, and June 2019 in Rexburg Idaho at 3 meter spatial resolution derived with the Direct resampling method and (b) R² values between VVIs and wheat LAI.

TABLES

Table 1-1 Sampling dates, crop type, soil texture and crop growth stage for five UAV data collection events that occurring at two Idaho field locations.

LOCATION	DATE	CROP	SOIL TEXTURE
Grace, ID, USA	May 30 2019	Winter Wheat	Silty Clay Loam
Grace, ID, USA	June 25 2019	Winter Wheat	Silty Clay Loam
Grace, ID, USA	July 8 2020	Winter Wheat	Silty Clay Loam
Rexburg, ID, USA	May 31 2019	Spring Wheat	Silt Loam
Rexburg, ID, USA	June 26 2019	Spring Wheat	Silt Loam

Table 1-2 the abbreviations, names, formulas, and references for twelve visible vegetation indices (VVI) that were evaluated.

VVI	Name	Formula	Reference
GLI	Green Leaf Index	$(2g-r-b)/2g+r+b$	Louhaichi et al.
VARI	Visible Atmospherically Resistant Index	$(g-r)/(g+r-b)$	Gitelson et al.
NGRDI	Normalized Green-Red Difference Index	$(g-r)/(g+r)$	Tucker
ExG	Excess Green Vegetation Index	$2g-r-b$	Woebbecke et al.
ExR	Excess Red Vegetation Index	$1.4r-g$	Meyer et al.
ExB	Excess Blue Index	$1.4b-g$	Mao et al.
ExGR	Excess Green minus Excess Red Vegetation Index	$ExG-ExR$	Neto et al.
MGRVI	Modified Green Red Vegetation Index	$(g^2-r^2)/(g^2+r^2)$	Tucker
WI	Woebbecke Index	$(g-b)/(r-g)$	Woebbecke et al.
IKAW	Kawashima Index	$(r-b)/(r+b)$	Kawashima et al.
RGBVI	Red Green Blue Vegetation Index	$(g^2-b*r)/(g^2+b*r)$	Bendig et al.
VEG	Vegetative Index	$g/(r^a b^{(1-a)})$, $a=0.667$	Hague et al.

Table 1-3 Descriptive statistics of leaf area index (LAI) measured at two locations and five events including the number of samples, the minimum (min), maximum (max), mean, standard deviation (SD), and the coefficient of variation (CV).

Location	Date	Samples	Min	Max	Mean	SD	CV
Training Data Set							
Rexburg	May 31 2019	43	0.24	1.04	0.51	0.18	36.40%
Rexburg	June 26 2019	43	2.88	5.35	4.09	0.59	14.34%
Grace	May 20 2019	67	0.10	3.07	0.94	0.54	57.52%
Grace	June 25 2019	67	0.75	5.45	2.74	1.00	36.69%
Grace	July 8 2020	29	0.78	4.30	1.98	0.93	47.06%
	All Dates	249	0.10	5.45	2.01	1.45	72.03%
Test Data Set							
Rexburg	May 31 2019	23	0.16	0.89	0.42	0.15	35.95%
Rexburg	June 26 2019	23	2.79	4.88	3.88	0.51	13.19%
Grace	May 20 2019	33	0.13	1.81	0.88	0.36	41.07%
Grace	June 25 2019	33	0.89	5.96	2.72	0.95	34.85%
Grace	July 8 2020	21	0.50	2.72	1.48	0.59	39.87%
	All Dates	133	0.13	5.96	1.87	1.37	73.03

Table 1-4 Model summaries for three leaf area index estimation models that predict leaf area index at the highest accuracy levels.

VVI	Spatial Res.	Resampling	Model Equation	R²	RMSE
NGRDI	3 meters	Ladder	LAI=17.14*NGRDI+1.76	0.66	0.73
MGRVI	3 meters	Ladder	LAI=8.63*MGRVI+1.76	0.66	0.73
VARI	3 meters	Ladder	LAI=14.02*VARI+1.81	0.66	0.74

SUPPLEMENTAL MATERIAL

The PAR measured by the AccuPAR within a plant canopy is a combination of radiation transmitted through the canopy and radiation scattered by leaves within the canopy. A complete model of transmission and scattering is given by Norman and Jarvis (1975), but it is very complex and not suitable for inversion. The Norman-Jarvis model suggested an equation for predicting scattered and transmitted PAR (equation 1).

$$\tau = \exp \left\{ \frac{A(1 - 0.47f_b)LAI}{\left(1 - \frac{1}{2K}\right)f_b - 1} \right\}$$

Equation 1.

This equations predicts canopy PAR within a few percent of values from the complete Norman-Jarvis model. When inverted the equation can be solved for LAI (equation 2).

$$LAI = \frac{\left[\left(1 - \frac{1}{2K}\right)f_b - 1\right] \ln \tau}{A(1 - 0.47f_b)}$$

Equation 2.

Where $A=0.283+0.785a-0.19a^2$, $K=\frac{1}{2\cos\theta}$ (where θ = Zenith angle of the sun), f_b = the fraction of incident of PAR which is beam, τ = ratio of PAR measured below the canopy to PAR above the canopy, and where LAI is leaf area index.

CHAPTER 2

Spatial Variability of Leaf Area Index from Drone Imaging of Two Irrigated Wheat Fields

Austin Paul Hopkins, Elisa Woolley, Ryan Jensen, Bradley Geary, Neil Hansen
Department of Plant and Wildlife Sciences, Brigham Young University, Provo, UT
Master of Science

ABSTRACT

Leaf area index (LAI) is an indicator of crop and plant growth in agricultural and ecological research. LAI can be used to monitor nitrogen status or estimate crop yield and evapotranspiration (ET). The aim of this study was to evaluate use of a remotely sensed visible vegetation index to characterize the spatial variability of LAI within irrigated wheat fields. Variation of LAI was measured with a ceptometer on random nested grids at two sites with pre-determined management zones in 2019 and 2020. Coincident digital imagery was collected using a consumer-grade unmanned aerial vehicle (UAV). A visible atmospherically resistant index (VARI) LAI estimation model was applied to red, green, blue (RGB) UAV imagery using a ladder resampling approach from 0.06 m to 3 m spatial resolution. There was significant within-field spatial and temporal variation of mean LAI. For example, in May at the Grace, ID location measured LAI ranged from 0.21 to 2.58 and in June from 1.68 to 4.15. The relationship of measured and estimated LAI among management zones was strong ($R^2=0.84$), validating the remote sensing approach to characterize LAI differences among management zones. There were statistically significant differences in estimated LAI among zones for all sampling dates ($P=0.05$). We assumed a minimum difference of 15% between zone LAI and the field mean for

justifying variable rate irrigation among zones, a threshold that corresponds with approximately a 10% difference in evapotranspiration rate. Three of the five sampling dates had LAI differences that exceeded the threshold for at least one zone, with all three having mean LAI of less than 2.5. The VARI model for estimating LAI remotely is more effective at identifying LAI differences among management zones at lower LAI.

INTRODUCTION

Leaf area index (LAI), defined as total upper leaf surface area divided by the corresponding land area (Chen et al 1992, Boegh 2002), is a valuable biophysical vegetation assessment (Watson, 1947). LAI is commonly used for estimating the rate of photosynthesis (Wells, 1991), plant productivity (Loomis and Williams, 1963), and water utilization (Richards and Townley-Smith, 1987). LAI can also be used for crop diagnostics, biomass estimation, and yield prediction (Duchemin et al., 2008). This study was motivated by the potential for measuring LAI to refine variable rate irrigation (VRI) recommendations within irrigated fields (King et al. 2002; Sadler et al. 2005). These VRI systems have potential for increasing water use efficiency in precision agriculture (West et al. 2017). Irrigation scheduling based on energy balance approaches commonly estimate crop evapotranspiration (ET_c) using a uniform crop coefficient (K_c) for the entire field. However, if significant spatial variation in LAI exists between zones, this would justify use of zone-specific crop coefficients and could lead to improved ET estimation for VRI prescriptions (Trout and Johnson, 2008, 2012; Evans et al. 2013; Hedley et al. 2009).

Remote sensing approaches to estimate LAI at various scales are more suitable than for precision agriculture applications than traditional methods of informing agricultural decisions. While remote sensing of LAI with satellites or other airborne platforms have been conducted at regional or global scales (Liang 2015, Li 2016, Dong 2019), fewer studies have evaluated remote sensing for evaluating the variation of LAI within irrigated fields (Neale et al 2012). While high altitude remote sensing via satellites can be useful (Knipper et al 2019), these systems can also have limitations. When applied at smaller scales, satellite or high atmosphere monitoring systems can be variable and unreliable due to confounding weather such as clouds, fog, haze, etc. In addition to weather, finer scale estimates of LAI can be limited by the spatial and temporal resolutions of satellites images. LAI can be measured manually with various time-consuming and labor-intensive methods, including point-measurements with a ceptometer (Yao 2008, Li 2019). To overcome the shortcomings of satellite and high atmosphere imagery, precision agricultural applications have used ground based, non-imaging sensors such as the AccuPAR LP-80 ceptometer to measure the LAI of a 2 m square area. Other methods of measuring LAI by hand include destructive sampling an entire measured area of interest and scanning the leaves to calculate how much area they take up compared to the area of the sample. These methods of measurement and estimation can be costly and have been shown to exhibit high degrees of spatial variation even in relatively uniform fields (Longchamps, 2015). Crop canopy sensing challenges associated with satellite based or non-imaging sensors may be partially overcome through use of Unmanned Aerial Vehicles (UAVs).

The development and application of Unmanned Aerial Vehicles (UAVs) in remote sensing (RS) have already shown their utility for precision agriculture in areas like fertilizer estimation, crop yield estimates, weed detection and general management. Likewise, they show

promise for applications related to improved irrigation management, including evapotranspiration (ET) estimation and variable rate irrigation (VRI) management/zone delineation. UAVs and other remote sensing technology provide direct benefit to precision agriculture managers. These systems have not yet reached their full potential and could be useful in describing within-field variation of LAI among other uses. UAVs are inexpensive, easy to operate, and managers can fly them as their needs dictate. Li et al. 2019 found that by combining color indices and textures of UAV imagery, in addition to the application of neural networks, they could reasonably estimate LAI remotely. However, the process of image acquisition and data analysis they used is complex and a simplified method of estimation would have value for increased accessibility and use in precision agriculture applications. Yao et al. 2017 also found that they could predict LAI in wheat with VVIs with a high accuracy of estimation with newly developed LAI model with modified triangular vegetation index (MTVI2) across a large range of LAI values (2-7). Their LAI model displayed performance under difference sub- categories of growth stages, varieties, and eco sites, pointing to LAI model estimation versatility. While spectral information and vegetation indices (VIs) derived from UAV-based multispectral or hyperspectral data are available for crop monitoring (Yue 2018, Xu 2019), these techniques and equipment are limited by their high cost and complexity of data analysis. This study evaluates use of visible vegetation indices derived from consumer grade UAVs to detect variation of wheat LAI within irrigated fields.

Hopkins 2021 et al showed the potential of estimating LAI using visible vegetation indices derived from images taken with consumer grade UAVs equipped with standard RGB digital cameras. They evaluated combinations of twelve VVIs, six spatial resolutions, and two data resampling methods and determined that the visible atmospherically resistant index (VARI)

model resampled through the ladder data resampling method (Hopkins 2021) at 3 m spatial resolution produced reasonable estimates of LAI. This study applies the method developed by Hopkins et al. (2021) to characterize variability of LAI among VRI zones of two irrigated wheat fields.

The objectives of this research are to determine if within-field variation of LAI can accurately be measured using UAV imagery; observe and detect spatial variation of LAI between pre-determined management zones; and ascertain if differences among zones meets a minimum threshold justifying variable rate irrigation. It is hypothesized that UAV measured within-field variation of LAI would coincide accurately with ceptometer measured LAI. In addition, spatial variation between pre-determined management zones could be detected and would exceed the minimum threshold justifying the application of VRI.

MATERIALS AND METHODS

Site Description

This study was conducted using five data collection events during the 2019 and 2020 growing seasons at two locations, Grace, ID and Rexburg, ID. The Grace, ID location (42.60904, -111.788, 1687 m above sea level) is a 22-ha field of irrigated winter wheat that is managed in a wheat-wheat-seed potato (*Solanum teberosum* L.) crop rotation. The soil at the Grace location is a Rexburg-Ririe complex with 1 to 4 percent slopes and a silty-clay-loam texture. Rexburg and Ririe soils are both coarse-silty, mixed, superactive, frigid Calcic Haploxerolls with 5 percent rock outcroppings that derive from alluvial influenced loess. Average annual precipitation is 355 mm with the majority of the precipitation falling as snow in the spring and winter months. Average annual temperature is 6.1 C and there are 80-110 frost-free days during the growing

season. Irrigation is applied using a 380 m center-pivot sprinkler system equipped with variable rate irrigation technology (Growsmart Precision VRI, Lindsay Zimmatic, Omaha, NE, USA).

The Rexburg, ID location (43.800752, -111.790064, 1518 m above sea level) is a wheat production field with a crop rotation of wheat and alfalfa. The study at this site was conducted on spring wheat (*Triticum Aestivum* L.) grown on a 22.7 ha field. The soil is a combination of Pocatello Variant silt loam and a Ririe silt loam with 2-8 percent slopes. Pocatello and Ririe soils are coarse-silty, mixed, calcareous, frigid, Typic Xerorthents and coarse-silty, mixed, frigid, Calcic Haploxerolls. The dominant field features are a relatively steep rolling 17-m long slopes from the southern end to the northern end of the field and relatively shallow top soil. Average annual precipitation is 393 mm with the majority of the precipitation typically falling as snow in the spring and winter months. Average annual temperature is 6.6 C with an 80 to 100 frost-free day growing season. Irrigation is applied using a 370 m long center-pivot sprinkler equipped with variable rate irrigation technology (Growsmart Precision VRI, Lindsay Zimmatic, Omaha, NE, USA).

UAV Image Acquisition and Processing

A DJI Phantom 4 outfitted with a Sentera single NIR sensor and RGB camera was flown over the fields. The Phantom 4 Pro camera has a 2.54 cm CMOS with 20 M effective pixels. A 3 axis gimbal integrated with the inertial navigation system stabilized the camera during flight. The UAV followed automated flight paths created using DroneDeploy (DroneDeploy, 2020) that imaged the entirety of each field at 91.44 m above ground level (AGL) and also at 118.87 m AGL with at least 80% image side and end overlap in the flight paths. Images for Grace were collected May 31, 2019, June 26, 2019 and July 8, 2020, during optimum UAV operating times

(11:00 am-2:00 pm). Images for Rexburg were collected May 30, 2019 and June 25, 2019 during optimum UAV operating times (11:00 am-2:00 pm) (Table1). The data were processed in Web OpenDroneMap (ODM, 2020). All the individual photos of each field were imported into WebODM and Reviewed. WebODM then automated the stitching together of the separate images into a multiple orthomosaics of the imaged fields. These were exported as a GeoTIFF to be processed in ArcGIS Pro. The RGB images were acquired with a resolution of 3000x4000 pixels (Ground resolution: 0.06 m at 91.44 m height) and were saved with GPS location information in GeoTIFF format.

Leaf Area Index Measurement and Estimation

Leaf area index data were collected with an AccuPAR model LP-80 PAR/LAI Ceptometer (METER Group) at pre-determined geographic points within each field (100 points at Grace and 66 points at Rexburg, Figures 1 & 2)(Kerry et al. 2003). To measure LAI at each point, the operator collected a single baseline measurement of the photosynthetically active radiation (PAR) above the canopy. Then, the operator collected PAR measurements below the canopy in each of the four cardinal directions rotating around a single point. The ceptometer calculates LAI based on the above and below canopy PAR measurements along with other variables that relate to the canopy architecture and position of the sun (Boegh 2002). These variables are the zenith angle, a fractional beam measurement value, and a leaf area distribution parameter (Also known as χ) for a particular canopy. The calculation of LAI is done using the Norman-Jarvis model (METER Group manual).

Estimates of LAI from UAV images was done by first calculating the visible vegetation index VARI and then converting it to LAI. Hopkins et al developed an LAI estimation model

from the visible atmospherically resistant index (VARI) model as depicted in equation 1. In order to characterize the spatial variability of LAI throughout the entire wheat field this model formula was applied to UAV imagery that was taken on each sampling date.

$$\mathbf{LAI=14.02*VARI+1.81} \qquad \mathbf{Equation\ 1}$$

The VARI model equation was applied via “raster calculator” in ArcGIS Pro to each visible band (RGB) UAV image we collected from our fields. The spatial resolution of the imagery was resampled using the ladder resampling method to 3 m from the native resolution of 0.006 m. A single band raster layer was derived from the model that consisted of estimated LAI values for each pixel in the imagery. Outlier values were set to a value of 0 if less than 0 and 6 if they were greater than 6. This raster layer was converted to point data using the “raster to point” tool in ArcGIS Pro (ArcGIS desktop: Release 10, Redlands, CA, USA). Then the estimated LAI point data layers were exported from ArcGIS Pro as excel data files. These were then processed in a geospatial statistics program called SpaceStat (SpaceStat, BioMedware: Ann Arbor, MI, USA). The measured LAI layer was scale interpolated to the 3 m grid of the estimated LAI point data to allow comparisons of estimated LAI.

Leaf Area Index Variation among Predefined Management Zones

Management zones were created according to previous research for both the Grace and Rexburg locations based on historic yield, measured variation of soil moisture, and topographic features (Svedin 2018, Woolley 2020, Larsen 2021). Five zones were delineated at the Grace location and three at the Rexburg location. Although these zones were delineated for future VRI management, all the data in this study is obtained with uniform irrigation management to quantify the variation of LAI due to factors other than management.

Means of LAI measured with the ceptometer were calculated by zone using the 66 points in Rexburg and the 100 points in Grace. Means of the UAV estimated LAI were determined for each zone from 150 randomly selected points per zone. For each of the LAI measurement dates and locations, the mean values for both the ceptometer measured LAI and the UAV estimated LAI were calculated to illustrate the differences in the LAI for all zones, dates, and locations, the ceptometer measured LAI values were subtracted from the UAV estimated LAI values. A linear regression was used to compare the ceptometer derived LAI means with the UAV estimated LAI means for each sampling date and zone. An ANOVA was performed among zones for each sampling date and location on the UAV estimated LAI values. When ANOVA showed that there were significant differences TukeyHSD tests were run to identify which zones were significantly different from one another. In addition to determining statistical significance of differences among zones, we established a minimum threshold to indicate whether significant differences were meaningful from the practical perspective for variable rate irrigation (VARI) management. For the purpose of our study a practical difference for the grower represents a minimum difference between the zone LAI mean and the field LAI mean of 15%. The minimum LAI threshold of 15% was calculated based on a relationship between LAI and crop coefficient (Trout et al., 2008) and an assumption that at least a 10% difference in daily evapotranspiration rates would be needed to justify application of VRI. All statistical tests were performed using R version 4.0.4.

RESULTS

Spatial and Temporal Variability of Measured Wheat Leaf Area Index

The LAI was measured at all sample locations at both the Grace, ID and Rexburg, ID sites on multiple dates (Table 1). For the Grace, ID location on May 30, 2019, the field average measured LAI was 0.87 with values ranging from 0.21 to 2.58 and a standard deviation of 0.31. For the same Grace, ID location on June 25, 2019, the LAI averaged 2.67 with values ranging from 1.68 to 4.15 and a standard deviation of 0.39. The increase in average LAI between the two dates reflects the growth and development of the crop canopy. A third date of LAI measurements at the Grace, ID location occurred in the following year on July 8, 2020. On that date, average measured LAI was 1.76 with values ranging from 1.06 to 3.42 and a standard deviation of 0.52. There were two LAI measurement dates for the Rexburg, ID location. On May 31, 2019, average measured LAI was 0.47 with values ranging from 0.22 to 0.97 and a standard deviation of 0.12. On June 26, 2019 LAI averaged 3.97 with a range of 3.5 to 4.6 and a standard deviation of 0.24. The five LAI measurement days provided a wide range in average LAI values for comparison with UAV estimated LAI. Within-field variation of LAI was generally lower for the Rexburg, ID location than for the Grace, ID. When the measured values were interpolated to show the spatial patterns for the entire field, the interpolated LAI showed little consistency over time at the Grace, ID location (Figure 3 a,b,c) but were more consistent over time at the Rexburg, ID location (Figure 4 a,b).

Spatial and Temporal Variability of Estimated Leaf Area Index

The UAV estimated LAI values were calculated for every pixel in each field image at both the Grace, ID and Rexburg, ID sites corresponding to each LAI measurement date (Table 1). For the Grace, ID location on May 30, 2019, the field mean UAV estimated LAI was 1.13 with values ranging from 0 to 4.47 and a standard deviation of 0.63. For the same Grace, ID location on June 25, 2019, the UAV estimated LAI averaged 2.91 with values ranging from 0 to 6 and a standard deviation of 0.58. The increase in average LAI between the two dates reflects the growth and development of the crop canopy. A third date of UAV estimated LAI calculations at the Grace, ID location occurred in the following year on July 8, 2020. On that date, average UAV estimated LAI was 2.08 with values ranging from 0 to 3.89 and a standard deviation of 0.56. There were two UAV estimated LAI measurement dates for the Rexburg, ID location. On May 31, 2019, average UAV estimated LAI was 0.44 with values ranging from 0 to 1.81 and a standard deviation of 0.17. On June 26, 2019 UAV estimated LAI averaged 3.20 with a range of 0.19 to 4.34 and a standard deviation of 0.34. The five days of UAV imagery observation provide a wide range in average UAV estimated LAI values for comparison with measured LAI (Table 2). Within field variation of UAV estimated LAI was generally lower for the Rexburg, ID location than for the Grace, ID location. Spatial patterns of UAV estimated LAI show some minor consistency over time at the Grace, ID location (Figure 5 a, b, c) and were more consistent over time at the Rexburg, ID location (Figure 6 a, b). In figure 5a we can see that the VARI model is detecting actual variation in the crop canopy. There is a semicircle of darker red/orange running through the center of the field. In the pivot irrigation line at that location there is a leaky connection between two sections and as such that area tends to green up more quickly. On the left half of the figure 5a you can see a large circular pattern. This represents an area of the field

that was flooded due to runoff from the slope above and poor drainage. The wheat in that area of the field all had to be replanted and as such was more immature than the bulk of the field. We can also see where the VRI system switches irrigation rates and waters the turfgrass on the other half of the range of the pivot irrigation system. This area on the southern border of the image receives more water as it is turfgrass. We can detect higher LAI values on those border areas as well. Figure 5b show the LAI during the June sampling, we can easily detect the rock outcropping in the field where there is not wheat planted. These show up as small yellow circular areas while the majority of the field is a deeper orange representing much higher LAI values. The majority of the spatial variation at this time seems to have smoothed out as the crop matures. Figure 5c is from July 2020 in Grace and we can still see some of the previously mentioned features such as the leaky wheel tracks, the rock outcroppings. We can see that the east side of the field has lower LAI values than the center does.

In figure 6 a we can observe the patterns of UAV estimated LAI in Rexburg at the May sampling. The darker orange areas at the north west portion of figure 6a are at the base of the slope where it flattens out. The slope itself is more yellow representing lower LAI values and once you get to the more southern end of the field the LAI starts to increase again. The LAI seems to follow the elevation of this field. You can observe a dark orange line running from north to south through the middle of figure 6a. This line represents an area of the field that was double planted as the result of an equipment malfunction. There is twice as much vegetation in this strip and the model succeeds in detecting this trend. In figure 6b we can observe the maintenance road that runs to the in field pump house, we can see the wheel tracks that are absent of vegetation. There are still small amounts of severe spatial variation within the crop canopy itself but as a whole much of it has smoothed out as it did in the Grace field as well.

Management Zone Comparisons of Measured and Estimated Leaf Area Index

The mean LAI for the 5 zones in Grace and the 3 zones in Rexburg, across all sampling dates, was calculated. The measured LAI mean was based on the ceptometer sampling locations sorted by zones and the UAV estimated LAI mean was based on 150 random points selected from each zone. The total number of LAI measurement comparisons is 21, 5 zones across 3 dates in Grace and 3 zones across 2 dates in Rexburg. There was a strong linear relationship between measured and estimated LAI ($R^2 = 0.84$, Figure 7). The UAV estimated LAI consistently produced higher LAI values than the ceptometer measured LAI values recorded at the Grace field. In May the ceptometer LAI mean was 0.87 and the UAV mean was 1.13. In June the ceptometer mean was 2.67 and the UAV mean was 2.91. Likewise In July 2020 the ceptometer LAI mean was 1.76 while the UAV mean was 2.08. The over estimation trend of the model does not occur in the Rexburg field as well though. The ceptometer mean LAI in May at Rexburg was 0.47 and 0.44 for the UAV model. In June the ceptometer mean was 3.97 while the UAV mean was 3.20. These observations details the strength/power of the UAV estimated LAI model. The ceptometer sampling layout did not lend itself to reliable statistical analysis because of irregular numbers of sampling points among zones. Figure 7 shows that we can reasonably use the UAV estimated LAI as a measurement of actual within field LAI when examining the spatial variation of LAI within and among the zones in these fields.

The UAV estimated LAI model performs at the highest accuracy near the LAI 2 mark in figure 7. An LAI value of 2 represents a crop canopy that has substantial growth but has yet to close the canopy (Nielsen et al. 2012). Some visible soil is still present in the UAV imagery at this time. According to the 1:1 line in figure 7 the UAV model begins underperforming later in

the growing season, after the wheat passes an LAI of 2. The model also overpredicts earlier in the season slightly at lower LAI values <2.

Comparison of Estimated Leaf Area Index among Management Zones

Significant differences were observed in estimated LAI among management zones. For the Grace location in May 2019, there were significant differences among management zones ($p < 0.001$) with zones 1 and 4 having higher LAI than the other zones. On that date, the difference between the means of zone 4 and zone 5 and the field mean exceeded the assumed minimum threshold to justify VRI. For the Grace location in June 2019 there were significant differences among zones ($p < 0.001$), with differences between the following zone comparisons: 1>2, 4>2, and 4>5. Despite the significant differences observed on that date, none of the differences between zone means and the field mean exceeded the minimum threshold to justify VRI. For the Grace location in July 2020 there were significant differences among zones ($p < 0.001$) and all zone comparisons were significantly different except zones 1 and 5 and zones 3 and 4 were not different. On that date, the difference between the mean of zones 1 and 5 and the field mean exceeded the assumed minimum threshold to justify VRI.

There were significant differences at the Rexburg location for May 2019 ($p < 0.001$) with differences for all zone comparisons. On that date, the difference between the means of zones 1 and 3 and the field mean exceeded the assumed minimum threshold to justify VRI. There were also significant differences for June 2019 ($p < 0.001$) with differences for all zone comparisons except for 3:1 (Table 3). However, despite the significant differences observed on that date, none of the differences between zone means and the field mean exceeded the minimum threshold to justify VRI.

DISCUSSION

Spatial and Temporal Variability of Measured and Estimated Leaf Area Index

This study measured LAI for five dates using a ceptometer at random nested grids at two field locations and compared the results to estimated LAI derived from a VARI UAV LAI estimation model (Table 2) LAI obtained by the two methods were highly correlated (Figure 7), but there were differences observed between the two approaches. In Grace the UAV estimated LAI values were generally higher than the kriged and interpolated values (Table 2) were but were still in line with the range and pattern exhibited in the actual measured LAI (Figure 3 a,b,c & Figure 5 a,b,c). Rexburg UAV estimated values had a wider range in LAI than ceptometer LAI values. For May Rexburg actual and estimated means were very similar. However, in June Rexburg UAV estimated mean was roughly 0.8 units lower than measured and interpolated LAI (Figure 4 a, b & Figure 6 a, b). Some of the differences between the two approaches come from the different methods from which they were derived. The measured LAI values excluded border areas and rock outcroppings that exist in the fields naturally. The estimated LAI image is derived from visual band orthophotos which includes rock outcroppings, weed patches and border areas.

One key objective of this study was to quantify the spatial variation of LAI in irrigated wheat fields. From Table 2 we can observe a wide range of values across both fields at all sampling dates. This suggests that there is a need for a variable K_c (crop coefficient) when using variable rate irrigation systems and the penmen-monteith equation to determine irrigation requirements within field. In Grace Id the mean values for the whole field at all three sampling dates the UAV estimated LAI model is approximately 0.3 LAI units higher than the measured and interpolated values. In Rexburg the mean field LAI is similar from both methods with only a

difference of 0.03 LAI units. However there is a much larger difference in the opposite trend in June. Measured LAI was 3.97 while UAV estimated LAI was 3.20. The model in this case is under-predicting rather than overpredicting as it was in Grace. Considering the range of values present in both fields (0-6 LAI), it appears that the model is predicting LAI ranges within a reasonable range. There appears to be enough of a range in values here to warrant further investigation into how the crop canopy varies and if this is significant or not.

Predefined Management Zone Differences between Ceptometer Measured and Unmanned Aerial Vehicle Estimated Leaf Area Index

Prior research from Hopkins Chapter 1 has shown that the VARI model at 3 meters spatial resolution and resampled with the ladder method has the highest R^2 value to ceptometer LAI and the lowest root mean square error (RMSE) value when estimating LAI from visible band UAV imagery. Hopkins et al examined a range of spatial resolutions (0.06m-3 m) within the LAI estimation models attempting to find the optimum spatial resolution to resample the native data to. It was found that 3 m spatial resolution was the highest performing compared to the finer resolutions. While 3 m spatial resolution was found to be the highest performing, precision agriculture growers are unable to manage their land on such a fine scale. A larger scale division of the field would be more useful when estimating LAI to inform decisions in precision agriculture. The management zones for Grace and Rexburg were the obvious scale to use because growers already break their fields up in these relatively large zones and treat them separately. Calculating the mean LAI of the management zones from the 3 m pixels LAI value may prove more useful than only calculating the LAI to the 3 m spatial resolution.

At Grace in May the VARI model zone LAI values were all lower in mean than the ceptometer values. This trend of the VARI model predicting LAI values is similar in most of the sampling dates and zones with some exceptions where the VARI model predicts higher values than the ceptometer LAI values do. Zone 2 consistently produces the lowest differences between VARI model and ceptometer LAI values. In May zone 2 had a difference of 0.1, in June 0.13, and in July of 2020 a difference of -0.04 (Table 3). Zone 2 is the area that is west and below the ridge in the field (Figure 1). This area is at the bottom of the slope of the ridge that is more extreme than the east side. This area often receives more water due to slope run-off. The values of those differences are not extreme enough to say that estimated LAI from the modeling is not similar enough to use in precision agriculture application. A difference of 0.1 can be viewed as negligible in practical applications where the typical range in spatial variation is 2.5-5 units of LAI.

The zone with the largest consistent differences in Grace between UAV estimated and measured LAI values was zone 4. Zone 4 is to the east of the ridge but is on an eastward facing downward slope instead of a flatter area. It could be that the east facing aspect of the slope combined with the runoff of water on the slope itself into other areas is causing this area to have poor overall mean LAI predictions.

In Rexburg in May all the zone UAV LAI means were very similar to those measured LAI ceptometer. Zone 1 had a difference of 0.03, zone 2 was 0.02, and zone 3 was 0.07. Showing again that when the field is at a lower mean LAI value of less than 1 the VARI model estimates LAI more accurately. However in June in Rexburg the VARI LAI model begins to overpredict severely compared to Grace and to Rexburg in May. The UAV model overpredicted compared to the ceptometer values by a mean of 0.77 compared to Mays 0.03 mean difference between the

methods. The poorest predicting zone in Rexburg at the June sampling was zone 2 with a difference between measurement methods of 0.99. This is the part of the field with the steepest sloping area that faces northwest and slopes down from south to north (Figure 2). Zones 1 and 3 did not perform significantly better than zone 2 however. Zones 1 and 3 had differences of 0.81 and 0.69 respectively (Table 4). At the June 26 sampling date the Rexburg field had a mean LAI of 3.97 showing that remote measurement of LAI at higher mean LAI values is not as reliable at LAI values below LAI 2.

Generally, the UAV estimated LAI that was calculated using the VARI model was similar in value to the ceptometer measured LAI. In Grace May 30 2019 (Table 3) the UAV model estimated higher than actual LAI values with the exception of zone 3 which had a difference of 0. Zone 2 also was high performing with a difference of only 0.1. The poorest performing zone in model estimation for this date is zone 4 which is above the sloping ridge that runs through the field. In Grace June 25 2019 three zones over predicted and two underpredicted but overall were similar in reasonable values. Zone 2 was the highest performing with the lowest difference (0.13). Zone 4 was again the poorest performing with the highest difference between LAI methods with a difference of 0.48. In Grace July 8 2020 most zones over-predicted although two underpredicted. Zone 2 was the most accurate with a difference of only 0.04. Zone 3 on the slope was the poorest predicted at a difference of 0.74. Although the difference in Grace July 8 2020 were much higher than in the other Grace sampling dates. The VARI model appears to have the greatest success earlier in the growing season prior to canopy closure.

In Rexburg May 31 2019 (Table 4) the differences were minimal between UAV estimated and measured LAI. The lowest difference zone was zone 2 with a value of 0.02 and the highest difference was 0.07 in zone 3. The VARI model predicts LAI accurately in the earlier stages of

the growing season as well. In Rexburg June 26 2019 (Table 4) the lowest difference is zone 3 with a value of 0.69 and the largest difference in zone 2 with a value of 0.99. This trend also matches what was observed in Grace. The success of the VARI model at predicting LAI appears to taper off as the growing season progresses and the wheat canopy begins closing. This could be a limitation of the visible band imagery being unable to penetrate past the observable layers and accurately detect the amount of crop canopy below what is readily observable.

We needed to determine if the UAV estimated LAI was reliable similar to the ceptometer measured LAI. A scatterplot (Figure 7) of the mean value of LAI for each zone with each method was created. This scatterplot compares the ceptometer measured LAI and the UAV estimated LAI. With the 3 m spatial resolution model used in Hopkins et al the VARI model had an R^2 of 0.66. However when expanded to represent the mean LAI values of the management zones the best fit line of the scatterplot had an R^2 of 0.84. This confirms the decision to apply the VARI model at a much larger, more easily managed spatial scale such as the management zones. This is in line with what Li et al 2019 found in their color indices estimation of leaf area index in rice research. They found their VARI model, when compared with measured LAI, had an R^2 of 0.74 and an RMSE of 1.13. Li et al did not include large management zone means in their research so the addition of that in this paper appears to have increased the efficacy of the VARI model. The UAV estimated LAI values are similar enough in values and nature to warrant further statistical exploration as the ceptometer LAI data did not have enough sampling points in every zone to be relied upon for ANOVA and Tukeys Post-Hoc tests. Further research could focus on combing the VARI model for estimating LAI remotely with a combination of bare soil imagery and mid-season digital surface/elevation models. This would examine the differences

between elevation values between bare soil imagery and the elevation of the crop canopy mid-season to better fill the gaps in the inefficiencies of the VARI model when estimating LAI.

Significant Differences between Predefined Management Zones of Unmanned Aerial Vehicle Estimated Leaf Area Index

It has been established that the VARI model based upon UAV imagery can reliably estimate LAI values within a reasonable range to the ceptometer measured values (Figure 7). The ANOVA tests revealed that there were statistically significant differences between at least some of the zones in each sampling date. The Tukeys tests revealed what zones were significantly different from one another.

The temporal variation trend continues in the results of the Tukey tests. In tables 3 & 4 the Tukeys test results for the zonal comparisons of mean LAI by zone. In May 30 2019, 6 out of the 10 zonal comparisons were statistically significantly different. Whereas in June 25 2019 in Grace only 3 out of the 10 zonal comparisons were significant. Likewise in Rexburg May 31 2019 all 3 of the zonal comparisons were significant. However in June 26 2019 at Rexburg only 2 out of the 3 zonal comparisons were significantly different. This trend demonstrates that there is greater spatial variation in the crop canopy of wheat earlier in the growing season. We cannot include the July 8 2020 observations in the discussion of temporal variation due to the lack of earlier season sampling that year.

Minimum Threshold Assumed to use Variable Rate Irrigation among Predefined Management Zones in Mean Leaf Area Index

Although the ANOVA and Tukeys post-hoc tests revealed statistically significant difference between the zones at all sampling dates, not all of these differences may be meaningful to growers. Variable rate irrigation systems and other forms of precision agriculture provide the ability to manage areas of the field individually, but this is limited by the physical nature of the crop management systems such as boom length, spray nozzle width, water flow rate, among others.

Although the ANOVA tests revealed significant differences in each sampling date in this research, not all of those differences are meaningful to growers however. A minimum threshold is set to assume the justification of the use of variable rate irrigation systems that would be meaningful to a grower. In this case, we determined that a management zone LAI mean must differ from the field LAI mean by a magnitude equal or greater than a 15% difference as that represents a 10% change in ET. This is based on the equations found in prior research that demonstrates how to convert LAI to K_c and then into ET_a (Neale 1989, Trout 2008, Trout and Johnson 2012). A 15% difference in zone mean LAI from the field mean LAI would be meaningful to the grower because that represents a level of irrigation water that would be controllable via variable rate irrigation (VRI) system. In Tables 3 & 4 we observed the statistically significant zonal differences. All five sampling dates had at least one statistically significant zonal comparison in the results. However, when examined under the restriction of the 15% minimum threshold difference those results narrow.

In May Grace 30 2019 (Table 3) zone 4 had a 15% difference from the field mean LAI and zone 5 had a -25% difference from the field mean LAI. None of the other zones were above the

minimum threshold from the field mean. In Grace June 25 2019 none of the zones were above the minimum threshold from the field mean even though they did have statistical significance in the ANOVA tests. In Grace July 8 2020 zone 1 was above the threshold at -17% difference. Zone 5 as well was over the threshold at -18% difference from the field mean.

For Rexburg May 31 2019 (Table 4) zone 1 and zone 3 were the only zones to break the minimum threshold. Zone 1 had a difference of 20% and zone 3 had a difference of -18%. However at the Rexburg June 26 2019 sampling none of the zones exceeded the minimum threshold to justify the use of variable rate irrigation even though they were statistically significantly different in the ANOVA test results.

The temporal variation trends are visible in the VRI minimum threshold as well. Neither of the June sampling dates contained any zones over the threshold even though they did in May earlier in the season. While the July 9 2020 Grace sampling did have 2 zones that were above the VRI threshold, we don't have an earlier temporal reference to point to a decrease for that year. This demonstrates when using UAVs to estimate spatial variation of within field LAI you are likely to find the most useful differences earlier in the growing season prior to canopy closure. The results point to the need of using a spatially variable crop coefficient (K_c) based upon UAV imagery when calculating the irrigation requirements of a field with variable rate irrigation systems. This is most applicable to wheat field that have yet to close the spaces between the rows with the canopy. It appears that after crop canopy closure the ET requirements become more uniform than earlier. Uniform enough that an irrigation manager may not be able to have a significant control on the different water requirements. Post canopy closure wheat fields could reliably use a uniform crop coefficient (K_c) when estimating irrigation water requirements from the Penmen-Monteith equation (Allen et al. 1998).

CONCLUSION

This study showed the potential of using the VARI leaf area index estimation model derived from UAV imagery to characterize spatial variation of LAI within an irrigated wheat field. There was significant variation detected within the fields of interest that ranged from 0.21 to 2.58 in May and 1.68 to 4.60 in June and July using the ceptometer in the field. From the UAV estimated LAI there was also a large range in LAI values ranging from 0-4.47 in May and 0-6 in June and July. The UAV based VARI model for estimating LAI is able to detect significant spatial variation of LAI within wheat fields similar to within field equipment monitoring of LAI. A linear comparison of zonal mean LAI of both methods of LAI measurement yields an R^2 value of 0.84 which was higher than Hopkins et al found in their examination of multiple models. The UAV based VARI model was able to detect statistically significant difference management zone mean LAI values across all sampling dates. A minimum threshold zone difference from the field LAI mean to justify the use of variable rate irrigation systems was determined to be a 15% difference of zone LAI from mean field LAI. Zones above the VRI threshold were detected by the UAV VARI model between zones in May at both sites (Grace: zone 4 15% and zone 5 -25%; Rexburg: zone 1 20% and zone 3 -18%) but none were detected in June at either site. In July of the following year there were practical differences detected in two of the zones (Grace: zone 1: -17% and zone 5: -18%) from the field mean. This demonstrates that while this remote detection of LAI is accurate, it is able to detect spatial variation of LAI more accurately prior to canopy closure of the wheat. These results also show the need of using a spatially variable crop coefficient (K_c) at times in the season when above the minimum threshold to justify the use of VRI systems among management zones. This variable K_c can be derived from the remotely

calculated LAI and used in the Penmen-Monteith equation to produce spatially variable water requirements. Future research should look into other variables that would increase the VARI models efficiency such as the addition of digital surface and elevation models comparing crop elevation to the bare soil elevation. These variables could include topographical features, soil physical properties and soil chemical properties potentially. Other questions that need to be addressed are how simple and data intensive management zones compare in precision agriculture efficacy.

LITERATURE CITED

- Allen, R. G., Pereira, L. S., Raes, D., & Smith, M. (1998). FAO Irrigation and drainage paper No. 56. *Rome: Food and Agriculture Organization of the United Nations*, 56(97), e156.
- Boegh, E., H. Soegaard, N. Broge, C. Hasager, N. Jensen, K. Schelde, and A. Thomsen. "Airborne Multi-spectral Data for Quantifying Leaf Area Index, Nitrogen Concentration and Photosynthetic Efficiency in Agriculture." *Remote Sensing of Environment* 81, no. 2-3 (2002): 179-193.
- Chen, J. M., & Black, T. A. (1992). Defining leaf area index for non-flat leaves. *Plant, Cell and Environment*, 15(4), 421–429. <https://doi.org/10.1111/j.1365-3040.1992.tb00992.x>
- Dong, T., Liu, J., Shang, J., Qian, B., Ma, B., Kovacs, J. M., Walters, D., Jiao, X., Geng, X., & Shi, Y. (2019). Assessment of red-edge vegetation indices for crop leaf area index estimation. *Remote Sensing of Environment*, 222, 133–143. <https://doi.org/10.1016/j.rse.2018.12.032>
- Duchemin, B., Maisongrande, P., Boulet, G., & Benhadj, I. (2008). A simple algorithm for yield estimates: Evaluation for semi-arid irrigated winter wheat monitored with green leaf area index. *Environmental Modelling & Software*, 23(7), 876–892. <https://doi.org/10.1016/j.envsoft.2007.10.003>
- Evans, R., J. LaRue, K. Stone and B. King. 2013. Adoption of site-specific variable rate sprinkler irrigation systems. *Irrigation Science* 31: 871-887.
- Hedley C. B. and I.J. Yule. 2009. A method for spatial prediction of daily soil water status for precise irrigation scheduling. *Agriculture Water Management*. 96: 1737-1745.
- Hopkins A. P. and Hansen N. C. 2021. Remote Sensing and Spatial Variability of Leaf Area Index Within Irrigated Wheat Fields. This Thesis

- Johnson, L. F., & Trout, T. J. (2012). Satellite NDVI Assisted Monitoring of Vegetable Crop Evapotranspiration in California's San Joaquin Valley. *Remote Sensing*, 4(2), 439–455. doi: 10.3390/rs4020439
- Kerry, R. and M. Oliver. 2003. Variograms of ancillary data to aid sampling for soil surveys. *Precision Agriculture* 4: 261-278.
- King, B. A., Reeder, R. E., Wall, R. W., & Stark, J. C. (2002). Comparison of Site-Specific and Conventional Uniform Irrigation Management for Potatoes. *2002 Chicago, IL July 28-31, 2002*. doi: 10.13031/2013.9171
- Knipper, K. R., Kustas, W. P., Anderson, M. C., Alsina, M. M., Hain, C. R., Alfieri, J. G., Prueger, J. H., Gao, F., McKee, L. G., & Sanchez, L. A. (2019). Using High-Spatiotemporal Thermal Satellite ET Retrievals for Operational Water Use and Stress Monitoring in a California Vineyard. *Remote Sensing*, 11(18), 2124. <https://doi.org/10.3390/rs11182124>
- Larsen, I., Hansen, N. C., Hopkins, B. G., Spatiotemporal Analysis of Variability in Soil Volumetric Water Content and Spatial Statistical Methods for Management Zone Delineation for Variable Rate Irrigation (2021) Brigham Young University Masters Thesis
- Li, X., Zhang, Y., Luo, J., Jin, X., Xu, Y., & Yang, W. (2016). Quantification winter wheat LAI with HJ-1CCD image features over multiple growing seasons. *International Journal of Applied Earth Observation and Geoinformation*, 44, 104–112. <https://doi.org/10.1016/j.jag.2015.08.004>
- Li, S., Yuan, F., Ata-Ul-Karim, S. T., Zheng, H., Cheng, T., Liu, X., ... Cao, Q. (2019). Combining Color Indices and Textures of UAV-Based Digital Imagery for Rice LAI Estimation. *Remote Sensing*, 11(15), 1763. doi: 10.3390/rs11151763

- Liang, L., Di, L., Zhang, L., Deng, M., Qin, Z., Zhao, S., & Lin, H. (2015). Estimation of crop LAI using hyperspectral vegetation indices and a hybrid inversion method. *Remote Sensing of Environment*, *165*, 123–134. <https://doi.org/10.1016/j.rse.2015.04.032>
- Loomis, R. S., & Williams, W. A. (1963). Maximum Crop Productivity: An Estimate 1. *Crop Science*, *3*(1), 67–72. <https://doi.org/10.2135/cropsci1963.0011183x000300010021x>
- Longchamps, L., R. Khosla, R. Reich, and D.W. Gui. 2015. Spatial and Temporal Variability of Soil Water Content in Leveled Fields. *Soil Science Society of America Journal* *79*: 1446-1454
- Manuals. (n.d.). Retrieved from <https://www.manualslib.com/products/Decagon-Devices-Accupar-Lp-80-8749930.html>
- Neale, C. M., Geli, H. M., Kustas, W. P., Alfieri, J. G., Gowda, P. H., Evett, S. R., ... Howell, T. A. (2012). Soil water content estimation using a remote sensing based hybrid evapotranspiration modeling approach. *Advances in Water Resources*, *50*, 152–161. doi: 10.1016/j.advwatres.2012.10.008
- Nielsen, D. C., Miceli-Garcia, J. J., & Lyon, D. J. (2012). Canopy Cover and Leaf Area Index Relationships for Wheat, Triticale, and Corn. *Agronomy Journal*, *104*(6), 1569–1573. <https://doi.org/10.2134/agronj2012.0107n>
- Sadler, E.J., R.G. Evans, K.C. Stone and C.R. Camp. 2005. Opportunities for conservation with precision irrigation. *Journal of Soil and Water Conservation* *60*:371.
- Svedin, Jeffrey David, “Characterizing the Spatial Variation of Crop Water Productivity for Variable-Rate Irrigation Management” (2018). All Theses and Dissertations. 6878. <https://scholarsarchive.byu.edu/etd/6878>
- Trout, T. J., Johnson, L. F., & Gartung, J. (2008). Remote Sensing of Canopy Cover in Horticultural Crops. *HortScience*, *43*(2), 333–337. doi: 10.21273/hortsci.43.2.333

- Watson, D. J. (1947). Comparative Physiological Studies on the Growth of Field Crops: II. The Effect of Varying Nutrient Supply on Net Assimilation Rate and Leaf Area. *Annals of Botany*, 11(4), 375–407. <https://doi.org/10.1093/oxfordjournals.aob.a083165>
- Wells, R. (1991). Soybean Growth Response to Plant Density: Relationships among Canopy Photosynthesis, Leaf Area, and Light Interception. *Crop Science*, 31(3), 755–761. <https://doi.org/10.2135/cropsci1991.0011183x003100030044x>
- West, G. and K. Kovacs. 2017. Addressing groundwater declines with precision agriculture: An economic comparison of monitoring methods for variable-rate irrigation. *Water* 9:28.
- Webster, R. and Oliver, M.A. 2001. *Geostatistics for Environmental Scientists* (John Wiley and Sons Ltd., Chichester, England)
- Woolley, E. A., Hopkins, B. G., Hansen, N. C., Soil water dynamics within Variable Rate Irrigation Zones for Winter Wheat. (2020) Brigham Young University Masters Thesis
- Xu, X. Q., Lu, J. S., Zhang, N., Yang, T. C., He, J. Y., Yao, X., Cheng, T., Zhu, Y., Cao, W. X., & Tian, Y. C. (2019). Inversion of rice canopy chlorophyll content and leaf area index based on coupling of radiative transfer and Bayesian network models. *ISPRS Journal of Photogrammetry and Remote Sensing*, 150, 185–196. <https://doi.org/10.1016/j.isprsjprs.2019.02.013>
- Yao, Y., Liu, Q., Liu, Q., & Li, X. (2008). LAI retrieval and uncertainty evaluations for typical row-planted crops at different growth stages. *Remote Sensing of Environment*, 112(1), 94–106. <https://doi.org/10.1016/j.rse.2006.09.037>
- Yao, X., Wang, N., Liu, Y., Cheng, T., Tian, Y., Chen, Q., & Zhu, Y. (2017). Estimation of Wheat LAI at Middle to High Levels Using Unmanned Aerial Vehicle Narrowband Multispectral Imagery. *Remote Sensing*, 9(12), 1304. doi: 10.3390/rs9121304

FIGURES

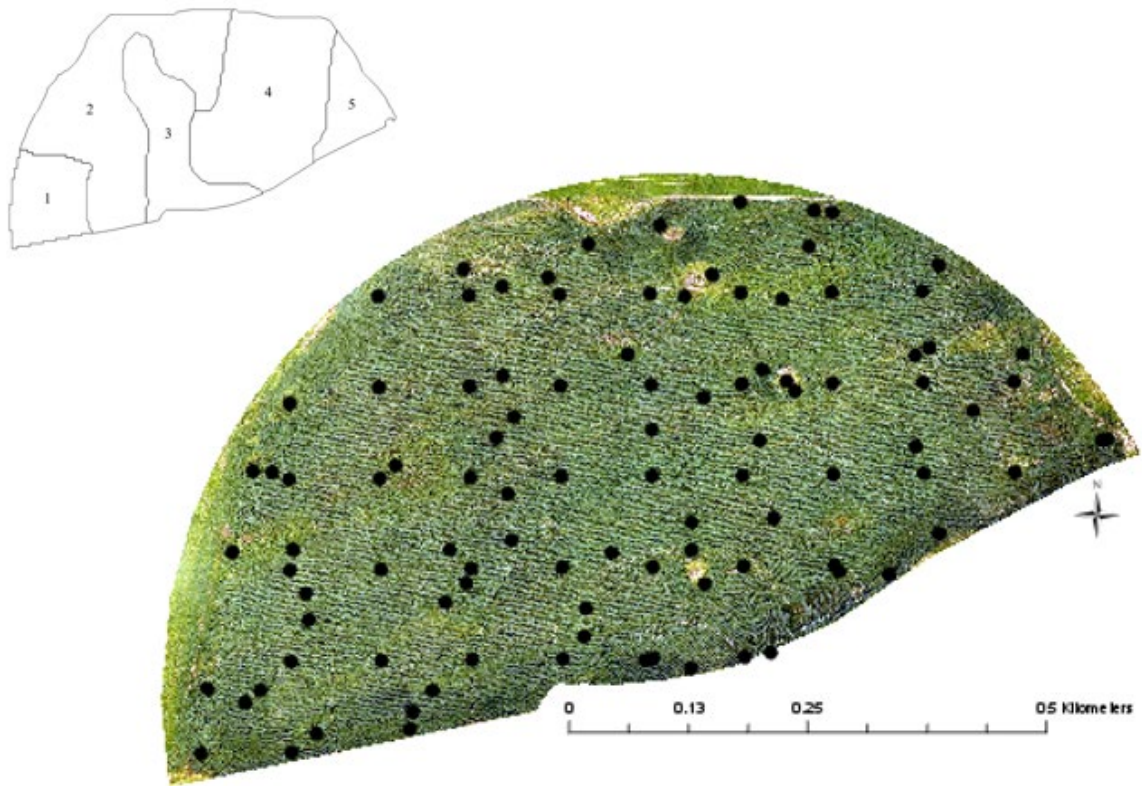


Figure 2-0-1 Aerial image from a UAV and map of sample points where leaf area index was measured with a ceptometer at the Grace, Idaho location. The inset figure shows the pre-determined management zones for this field.

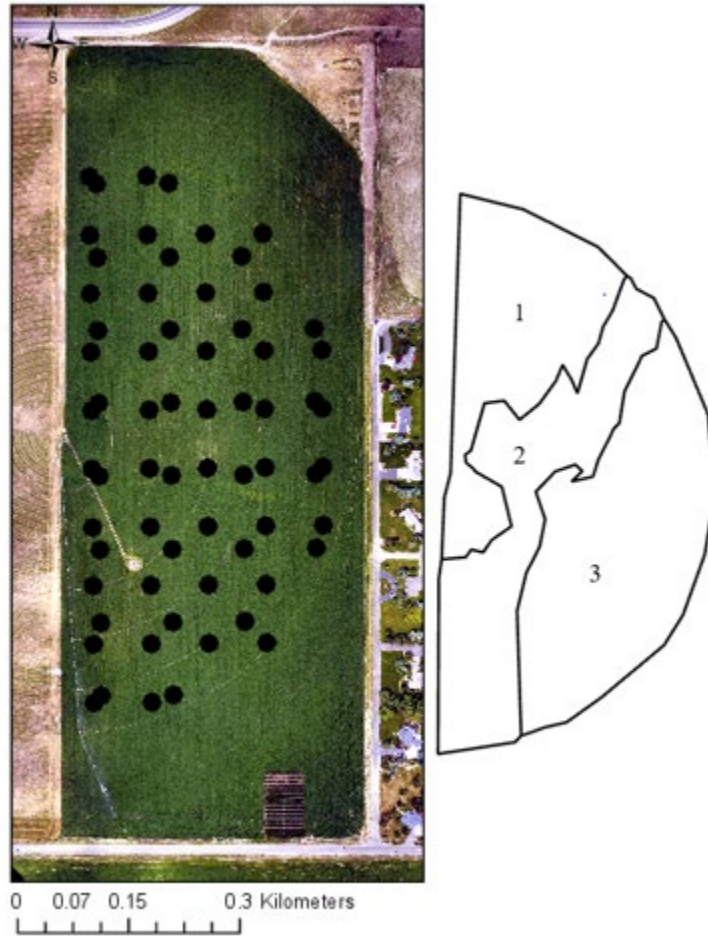


Figure 2-0-2 Aerial image from a UAV and map of sample points where leaf area index was measured with a ceptometer at the Rexburg, Idaho location. The inset figure shows the pre-determined management zones for this field.

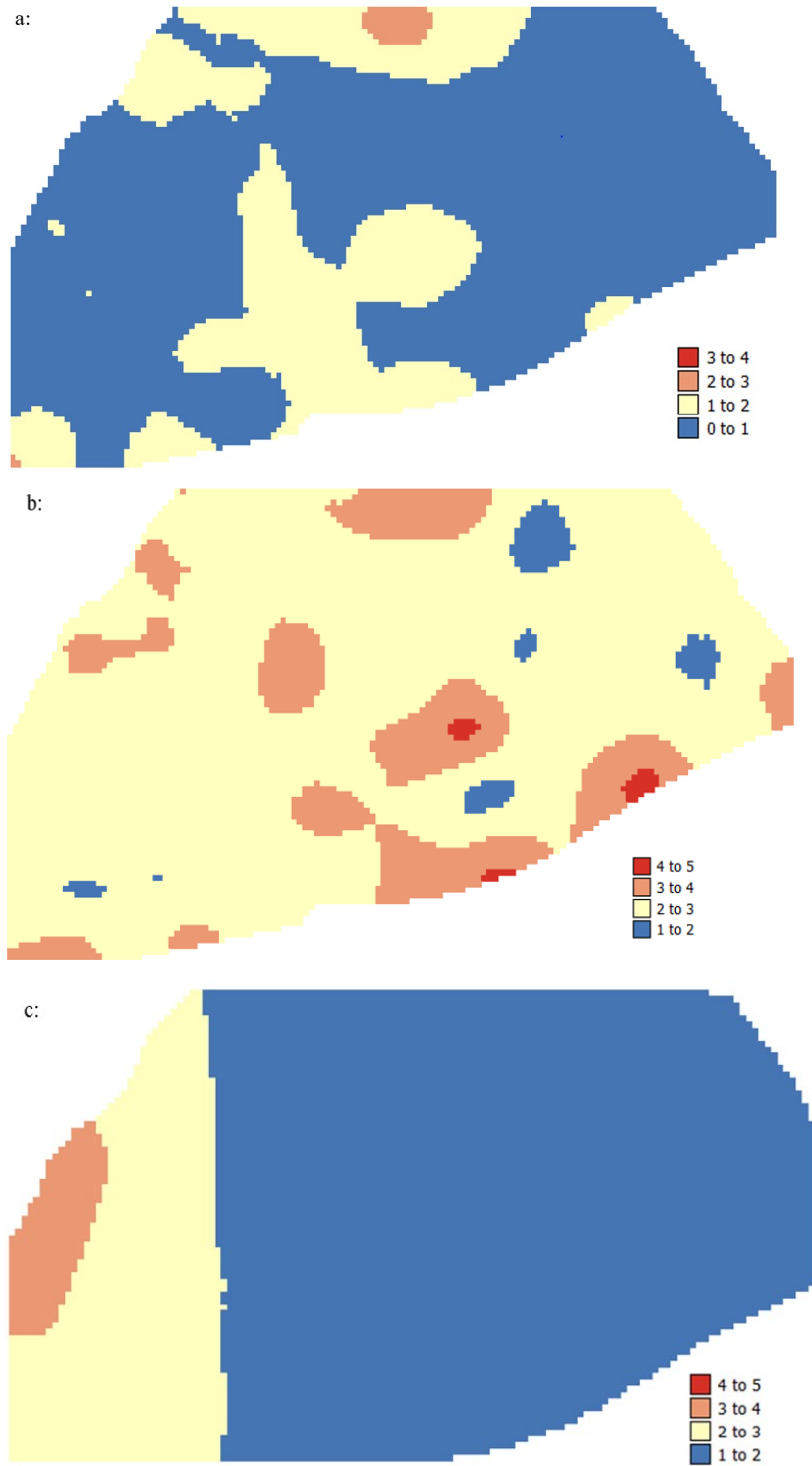


Figure 2-0-3 Leaf area index of the Grace, Idaho field location measured using a ceptometer on a: May 30, 2019, b: June 25, 2019, c: July 8, 2020 and spatially interpolated using Kriging.

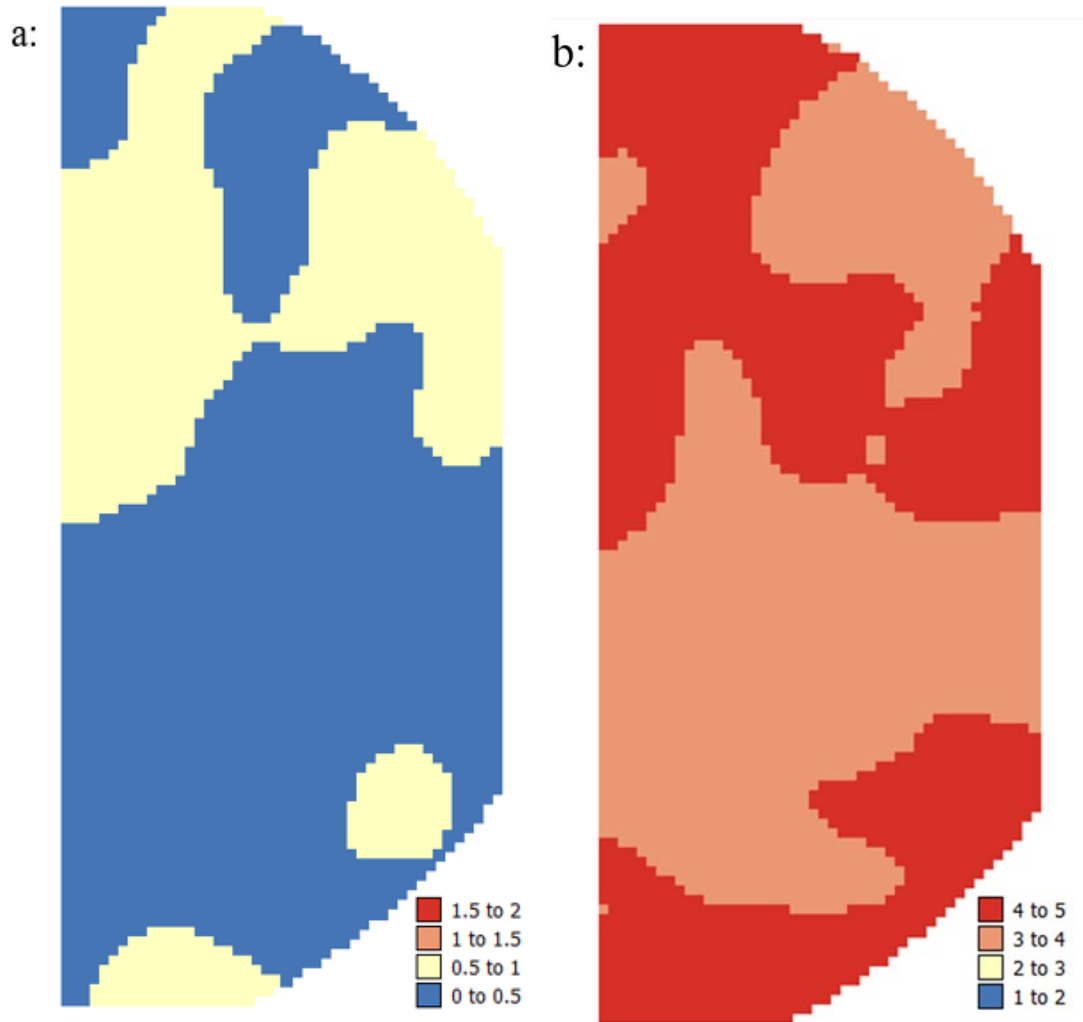


Figure 2-0-4 Leaf area index of the Rexburg, Idaho field location measured using a ceptometer on a: May 31, 2019 and b: June 26 and spatially interpolated using Kriging.

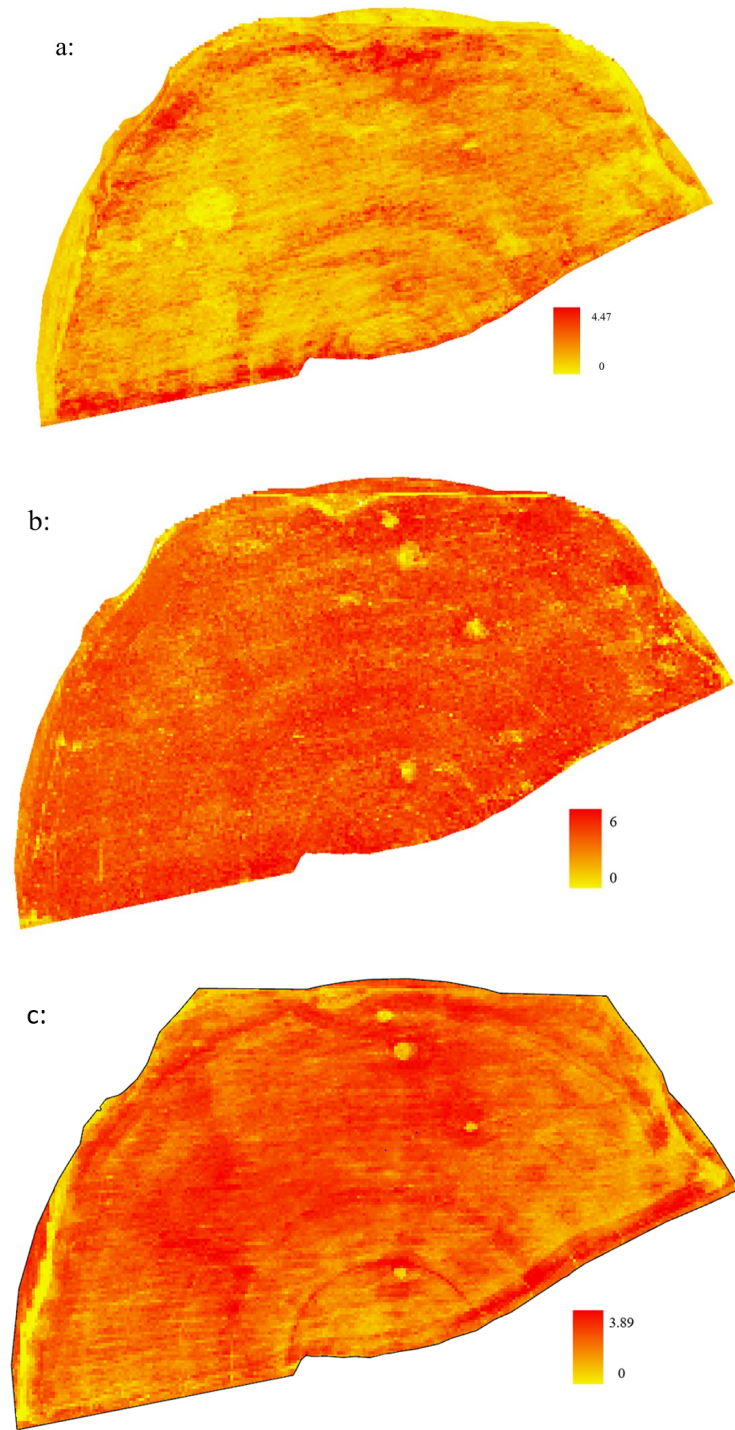


Figure 2-0-5 Raster images representing estimated LAI values for the Grace, Idaho field location on a: May 30 2019 b: June 25 2019 and c: July 8 2020 based on VARI model LAI estimation methods.

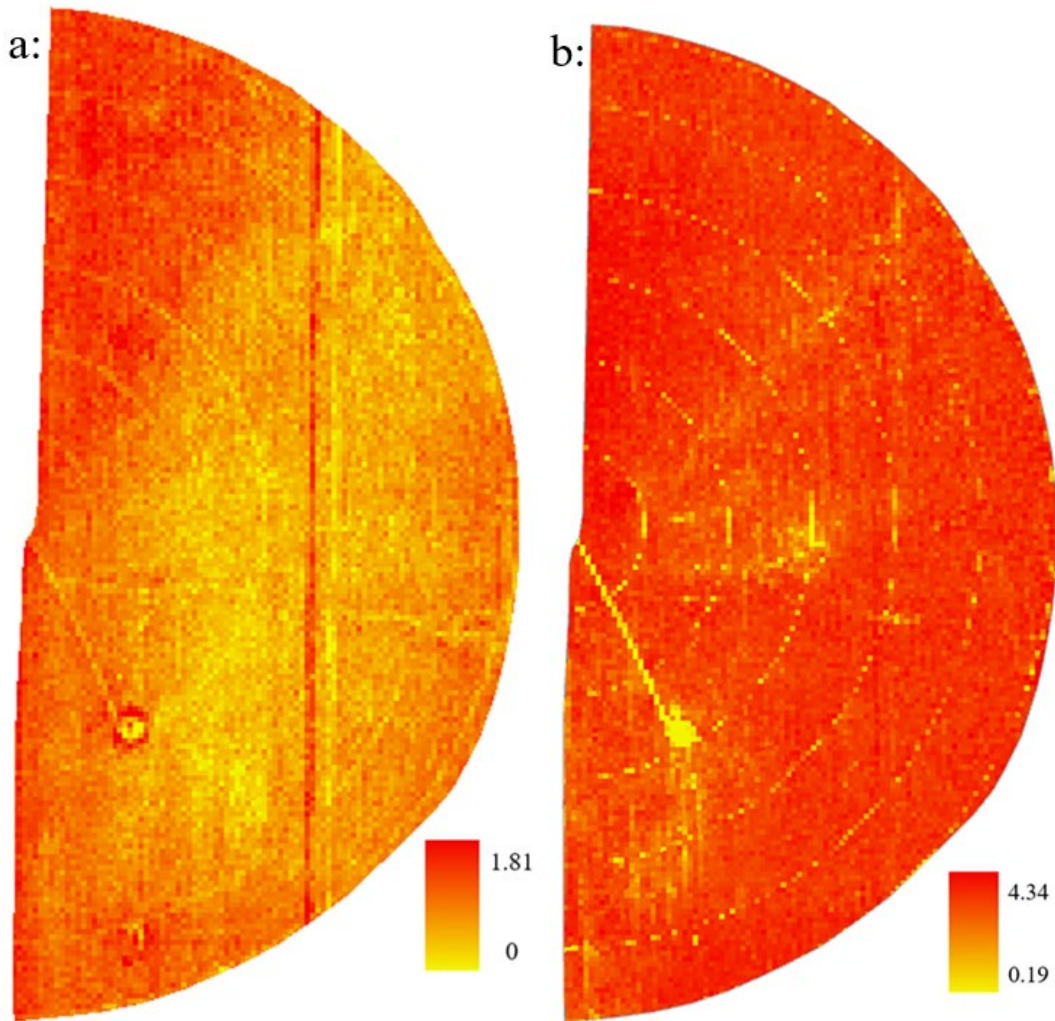


Figure 2-0-6 Raster image representing estimated LAI values for the Rexburg, Idaho field location on a: May 31 2019 and b: June 26 2019 based on VARI model LAI estimation methods.

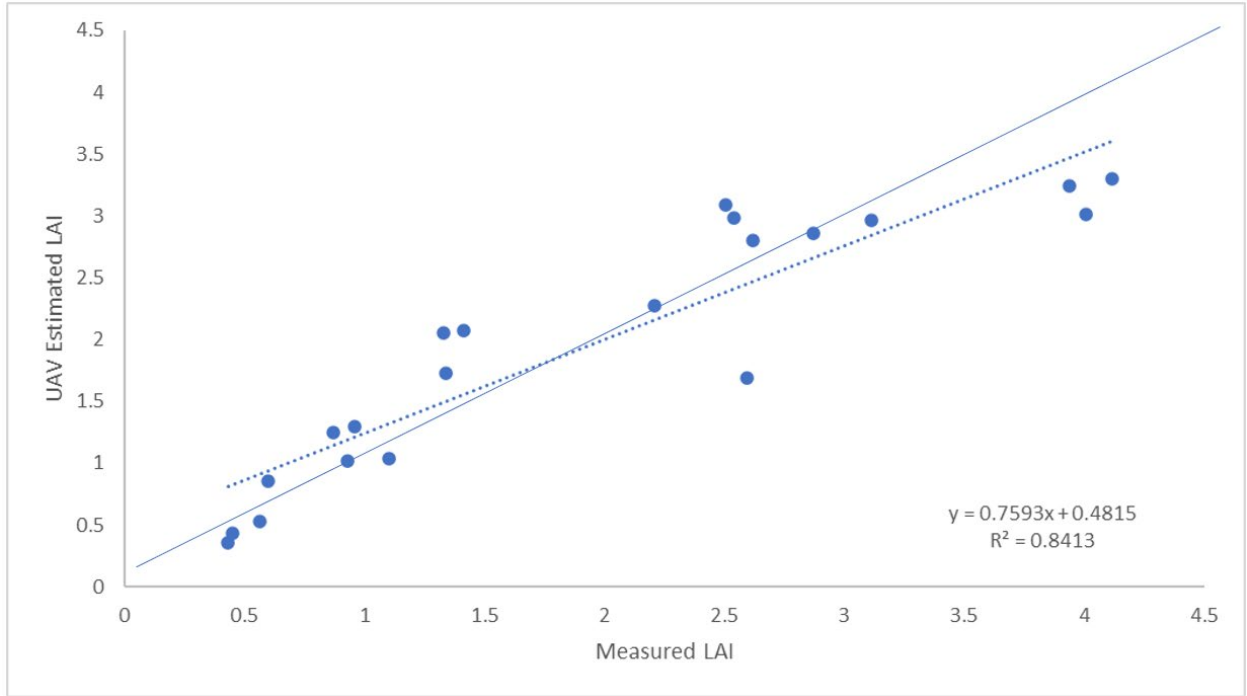


Figure 2-7 Scatterplot with fit line (dotted) and a 1:1 line (solid), R2 value, and regression equation of the comparison of the mean leaf area index (LAI) measured for each zone to the mean LAI estimated using a model derived from images taken with an unmanned aerial vehicle (UAV) for each zone using data from all sampling dates and both locations

TABLES

Table 2-1 Sampling dates, crop type, and soil texture for the two field locations. On these dates, LAI was measured on the ground using ceptometer readings and unmanned aerial vehicle (UAV) images were obtained for calculation of leaf area index.

LOCATION	DATE	CROP	SOIL TEXTURE
Grace, ID, USA	May 30, 2019	Winter Wheat	Silty Clay Loam
Grace, ID, USA	June 25, 2019	Winter Wheat	Silty Clay Loam
Grace, ID, USA	July 8, 2020	Winter Wheat	Silty Clay Loam
Rexburg, ID, USA	May 31, 2019	Spring Wheat	Silt Loam
Rexburg, ID, USA	June 26, 2019	Spring Wheat	Silt Loam

Table 2-2 Descriptive statistics of measured leaf area index (LAI) and unmanned aerial vehicle (UAV) estimated LAI measured on multiple dates at the Grace, ID and Rexburg, ID locations.

LOCATION	MIN	MAX	MEAN	ST. DEV
	-----LAI, m ² m ⁻² -----			
Measured LAI				
Grace May 2019	0.21	2.58	0.87	0.31
Grace June 2019	1.68	4.15	2.67	0.39
Grace July 2020	1.06	3.42	1.76	0.52
Rexburg May 2019	0.22	0.97	0.47	0.12
Rexburg June 2019	3.50	4.60	3.97	0.24
UAV Estimated LAI				
Grace May 2019	0	4.47	1.13	0.63
Grace June 2019	0	6	2.91	0.58
Grace July 2020	0	3.89	2.08	0.56
Rexburg May 2019	0	1.81	0.44	0.17
Rexburg June 2019	0.19	4.34	3.20	0.34

Table 2-3 Estimated leaf area index (LAI) values for the Grace, ID location averaged by date and management zone and the percent difference between management zone and field means. Estimated LAI means followed by the same letter do not significantly differ.

	Management Zone					Field Mean
	1	2	3	4	5	
May 30, 2019						
Estimated LAI m ² m ⁻²	1.15 a	1.05 bc	1.05 c	1.30 a	0.84 bcd	1.13
(Zone Mean - Field Mean) / Field Mean x 100	2	-7	-7	15*	-25*	-
June 25, 2019						
Estimated LAI m ² m ⁻²	2.93 acde	2.76 be	2.98 cde	3.07 d	2.78 e	2.91
(Zone Mean/Field Mean) x 100	1	-5	2	5	-4	-
July 8, 2020						
Estimated LAI m ² m ⁻²	1.72 a	2.27 b	2.07 c	2.12 cd	1.70 a	2.08
(Zone Mean/Field Mean) x 100	-17*	9	-1	2	-18*	-

* These management zone LAI means differ from the field LAI mean by a magnitude equal to or greater than the 15% minimum threshold assumed to justify the use of variable rate irrigation.

Table 2-4 Estimated leaf area index (LAI) values for the Rexburg, ID location averaged by date and management zone and the percent difference between management zone and field means. Estimated LAI means followed by the same letter do not significantly differ.

	Management Zone			Field Mean
	1	2	3	
May 31, 2019				
Estimated LAI m ² m ⁻²	0.53 a	0.43 b	0.36 c	0.44
(Zone Mean - Field Mean) / Field Mean x 100	20 *	-2	-18*	-
June 26, 2019				
Estimated LAI m ² m ⁻²	3.30 a	3.02 b	3.25 a	3.20
(Zone Mean/Field Mean) x 100	3	-6	2	-

* These management zone LAI means differ from the field LAI mean by a magnitude equal to or greater than the 15% minimum threshold assumed to justify the use of variable rate irrigation.